



Spatiotemporal trends of temperature and precipitation extremes across contrasting climatic zones of China during 1956–2015

Jing Zheng¹ · Junliang Fan^{1,2,3} · Fucang Zhang^{1,2}

Received: 23 April 2019 / Accepted: 1 July 2019 / Published online: 13 July 2019
© Springer-Verlag GmbH Austria, part of Springer Nature 2019

Abstract

Spatiotemporal changes of temperature and precipitation extremes from 1956 to 2015 were analyzed at 200 representative weather stations evenly distributed in the temperate continental zone (TCZ), temperate monsoon zone (TMZ), mountain plateau zone (MPZ), and (sub) tropical monsoon zone (SMZ) of China, using 16 extreme temperature and 11 extreme precipitation indexes. The results showed that warm days (TX90p) and warm nights (TN90p) increased significantly, while cool days (TX10p) and cool nights (TN10p) decreased significantly in the whole China. Overall increasing trends were found for maximum and minimum daily maximum temperature (TXx and TXn) and maximum and minimum daily minimum temperature (TNx and TNn). Warm indexes, including summer days (SU25), tropical nights (TR20), warm spell duration indicator (WSDI), and growing season length (GSL), showed increasing trends, whereas cold indexes such as frost days (FD0), ice days (ID0), cold spell duration indicator (CSDI), and diurnal temperature range (DTR) showed decreasing trends. These extreme temperature indexes exhibited high correlations with mean air temperature. MPZ exhibited the most remarkable change magnitudes among the four zones, while the smallest changes occurred in SMZ. An accelerating warming trend was particularly observed since 1986. Nationally, only daily rainfall intensity (SDII) showed significantly increasing trends, while the increasing trends of other precipitation indexes were not significant. Apart from consecutive wet days (CWD), changes of precipitation extremes presented increasing trends. PRCPTOT and R10mm exhibited the highest correlation coefficient across contrasting climatic zones. Regionally averaged precipitation totals were decreasing in TMZ during 1956–1985, but increasing trends were identified after 1985. The upward tendency of precipitation totals in MPZ and the west part of TCZ may alleviate the pressure of water shortage in arid and semi-arid regions of China, but the upward trend in SMZ, especially in the coastal areas of southeastern China, may aggravate the risk of flood-induced disasters in these regions.

Keywords Global warming · Temperature extremes · Precipitation extremes · RCLimdex · Mann–Kendall test

Electronic supplementary material The online version of this article (<https://doi.org/10.1007/s00704-019-02942-5>) contains supplementary material, which is available to authorized users.

✉ Junliang Fan
nwwfjl@163.com

- ¹ Key Laboratory of Agricultural Soil and Water Engineering in Arid and Semiarid Areas of Ministry of Education, Northwest A&F University, Yangling 712100, China
- ² Institute of Water-saving Agriculture in Arid Areas of China, Northwest A&F University, Yangling 712100, China
- ³ College of Water Resources and Architectural Engineering, Northwest A&F University, Yangling 712100, China

1 Introduction

The global mean surface temperature has enhanced approximately 0.85 °C during 1880–2012 (IPCC 2013), which is expected to rise by more than 1.5 °C in the late twenty-first century (2081–2100) compared with that between 1850 and 1900 (Pachauri et al. 2014). This condition is usually called “global warming,” and it is largely possible that the increase in warm extremes and decrease in cold extremes would take place in the twenty-first century around the whole world (Wang et al. 2018; Dookie et al. 2019). Extreme climate events (floods, heat waves, droughts, etc.) have the characteristics of difficult predictability and strong destructiveness, which play adverse roles on the socio-economic system and

terrestrial ecosystems (Cheong et al. 2018). Climate change will also affect plant development, insects, and final yields. In some regions, climate warming can benefit locally planted crops types, or shift farmers to crops that are currently grown in warmer areas. Rather, if the temperature is higher than the crop's optimum temperature, crop yields will decrease. Potential hazards to crop production are mainly attributed to water shortage and heat stress (Harrison et al. 2011). Warm-wet conditions can create favorable conditions for the growth of insect pests, improve its propagation speed, and indirectly affect the agricultural production (Castex et al. 2018). Therefore, it has been urgent to investigate the spatiotemporal trends and magnitudes of climatic extremes, so as to provide a basis for climate change studies, disaster risk assessment, and decision-making strategies.

China has a vast territory and is often influenced by a variety of climatic extremes. Over the past few decades, there have been many studies examining extreme climatic events in different regions of China to improve the in-depth understanding of the variations of extreme events, and build a bond for researchers to work on global climate change. The studied regions include the Tianshan Mountains (Xu et al. 2018), the Loess Plateau (Sun et al. 2016), the Tibetan Plateau (Liu et al. 2009), the Wei River Basin (Liu et al. 2018), the Yangtze River Basin (Guan 2015, Guan et al. 2015), the coast area of China (Wang et al. 2017), the monsoon region of China (Gao et al. 2017), northwestern China (Wang et al. 2013b), northeastern China (Yu and Li 2015), northern China (Mei et al. 2018), and southern China (Ding et al. 2018), etc. The results indicated that temperature extremes showed consistently upward trends, with large regional variations in various areas of China. However, changes of precipitation extremes across China are distinct due to the differences in regional characteristics, climatic background, and driving forces (Xu et al. 2011).'

In terms of time series, the rising of global mean surface temperature has accelerated after the mid-1980s (Yu and Li 2015). Studies by Shi et al. (2007) indicated that the climate in northwestern China began to vary from dryer to wetter in 1986. Jiang et al. (2012a) revealed that the majority of precipitation indexes in Xinjiang of China showed shifts starting from the mid-1980s. The climatic change among various climate zones of China before and after the 1980s may exhibit diverse trends and magnitudes. Comprehensively understanding the long-term trend and magnitude of climatic changes, as well as the abrupt change years across the whole China, is very essential. However, until now, it has been unclear how the climatic extremes changed in different climatic regions of China since the 1980s. On the other hand, in terms of climatic indexes, few indexes were usually adopted and these indexes applied by most studies were not consistent. All types of extreme indexes suggested by the Expert Team on Climate Change Detection and Indices (ETCCDI) can be used to

comprehensively evaluate the changes of climate extremes across a wide variety of climates. Consequently, the aims of the present study are as follows: (1) to analyze the temporal variations and spatial distributions of extreme temperature and precipitation indexes over the past six decades (1956–2015) across China using 27 extreme indexes proposed by ETCCDI; (2) to assess the differences in extreme indexes before and after the 1980s in different climatic zones of China responding to ongoing global warming. The study is crucial for understanding the regional and national climate changes and providing a guideline for associated scientists and policymakers to develop food production and eco-environment management strategies in contrasting climatic zones of China.

2 Materials and methods

2.1 Study area

The study area, i.e. the Mainland China excluding the Taiwan Province, Hong Kong, and Macao Special Administrative Regions due to the lack of meteorological data, is consisted of 22 provinces, five autonomous regions, and four municipal cities. The study area can be partitioned into five climate regions, the temperate continental zone (TCZ), the temperate monsoon zone (TMZ), the mountain plateau zone (MPZ), the subtropical and tropical monsoon zone (SMZ and TPMZ, respectively) (Fan et al. 2018; Fan et al. 2019). Considering that the tropical monsoon zone is much smaller than the other four climate zones, it was merged into the subtropical zone as the (sub) tropical monsoon zone in the present study (Fig. 1). The average annual precipitation in the four climatic zones is 269 mm, 585 mm, 382 mm, and 1320 mm, and the annual evaporation is 2148 mm, 1475 mm, 1883 mm, and 1545 mm. TCZ, TMZ, MPZ, and SMZ are classified as arid, semi-arid, semi-humid, and humid regions, respectively.

2.2 Data collection and extreme indexes selection

Daily minimum (T_{\min}) and maximum (T_{\max}) temperature and precipitation data during 1956–2015 at 200 meteorological stations across China were given by the National Meteorological Information Center of the China Meteorological Administration (<http://data.cma.cn/>), who has primarily controlled the meteorological data quality. The data quality was further controlled using the RCLimDex (version 1.8) software package, which was proposed by Zhang and Yang (2004). This software is able to identify all the missed or absurd data. Daily precipitation values smaller than zero or minimum temperature exceeding the maximum temperature was flagged as erroneous. The distributions of these

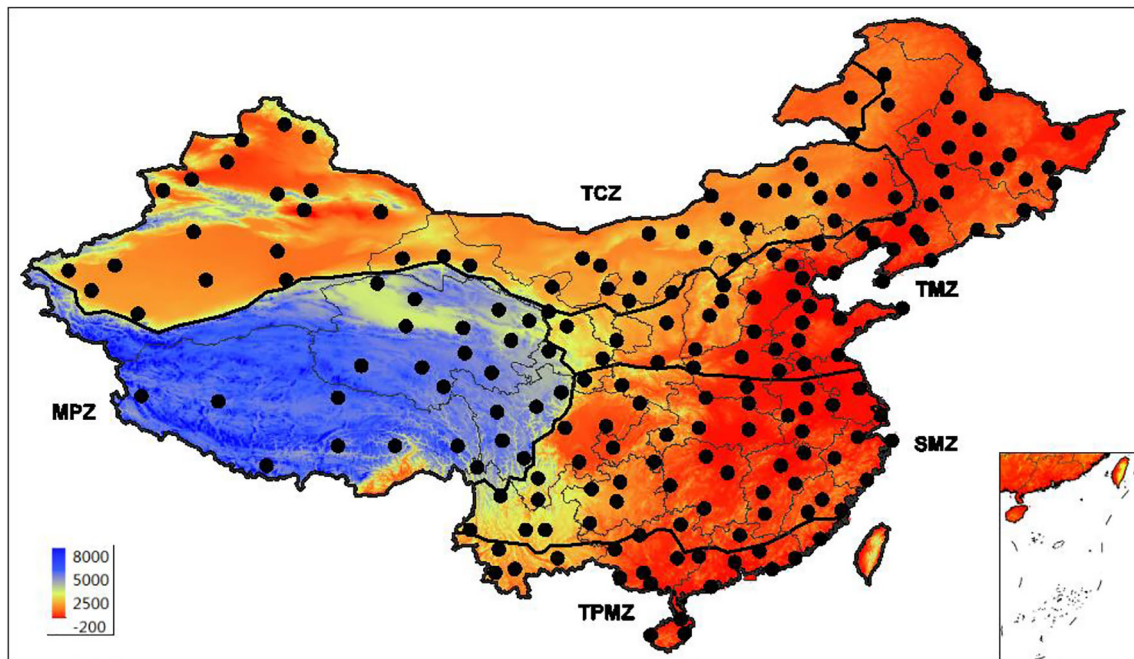


Fig. 1 Distribution of the five climatic zones across China and the geographical locations of the 200 weather stations selected in this study. TCZ: temperate continental zone; TMZ: temperate monsoon zone; MPZ:

mountain plateau zone; SMZ: subtropical monsoon zone; TPMZ: tropical monsoon zone

meteorological stations are as follows: 58 stations in TCZ, 49 stations in TMZ, 23 stations in MPZ, and 70 stations in SMZ.

All the 16 extreme temperature and 11 extreme precipitation indexes suggested by ETCCDMI were considered here, which were calculated based on daily T_{\max} , T_{\min} , and precipitation using the RClimDex software. The temperature indexes consisted of nine warm extremes and seven cold extremes, which were further grouped according to their calculation methods as four percentile-based indexes, four absolute indexes, four thresholds indexes, three duration indexes, and one other index. The precipitation indexes included 10 wet indexes and one dry index, which were further classified as two percentile, two absolute, three threshold, two duration, and two other indexes. The detailed definitions of these indexes please refer to previous studies (Alexander et al. 2006).

2.3 Trend analysis and abrupt change detection

The Sen's slope estimator (Sen 1968) was applied for calculating the long-term monotonic trends of climate extremes, which has been widely used to identify the trend of climatic and hydrological time-series variables (Gocic and Trajkovic 2013; Fan et al. 2016). The trends were computed during the whole period of 1956–2015 and also during two 30-year periods of 1956–1985 and 1986–2015. The non-parametric Mann–Kendall (MK) method was utilized to test the significance level of the change trend, which was proposed and improved by Mann (1945) and Kendall (1975). Positive Mann–Kendall Z values greater than 1.96 and 2.58 represent

significantly upward trend at a level of 0.05 and 0.01 respectively, while negative Z values lower than -1.96 and -2.58 represent a significantly downward trend. The non-parametric Pettitt test (Pettitt 1979) was broadly applied to examine the abrupt change point in climatic and hydrological observations, which was employed to here to detect the abrupt change years of the time-series temperature and precipitation extremes during 1956–2015. Correlation coefficients among the extreme indexes were detected and estimated by Pearson's correlation and the two-tailed t test (Rodgers and Nicewander 1988) using the SPSS 16.0 statistical software (SPSS Inc., Chicago, USA). The temporal variations and spatial distributions of climatic extremes were illustrated by R package and ArcGIS, respectively.

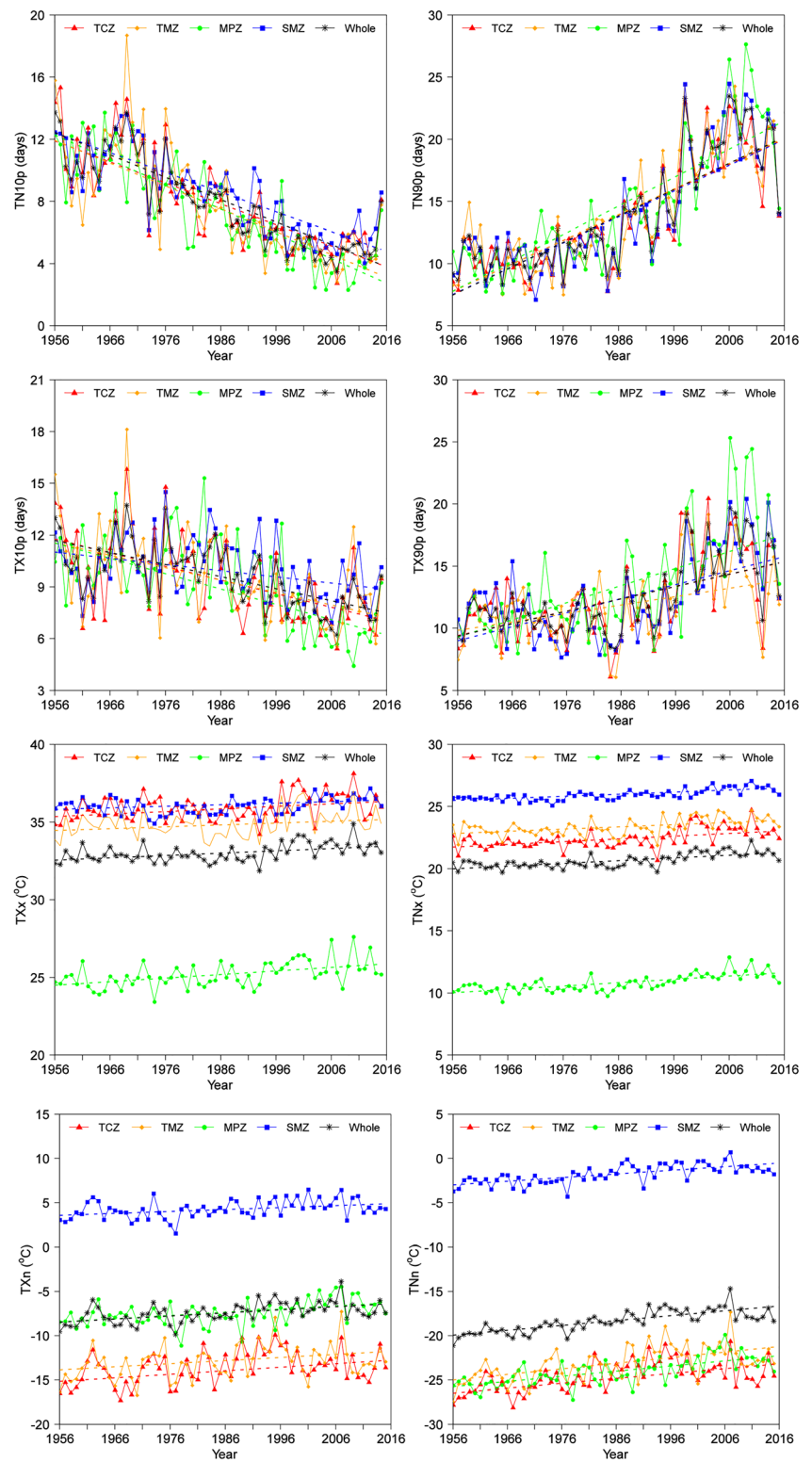
3 Results

3.1 Spatiotemporal changes of extreme temperature indexes

3.1.1 Percentile-based and absolute extreme temperature indexes (TN10p, TN90p, TX10p, TX90p, TXx, TNx, TXn, TNn)

Spatially averaged cool nights (TN10p) and cool days (TX10p) displayed an obvious decrease between 1956 and 2015 in contrasting climate zones of China, but warm nights (TN90p), warm days (TX90p), and all absolute indexes, i.e., maximum T_{\max} (TXx), maximum T_{\min} (TNx), minimum T_{\max}

Fig. 2 Annual variations of spatially averaged values of percentile-based and absolute temperature indexes during 1956–2015 across different climatic zones of China



(TXn), and minimum T_{\min} (TNn), showed increasing trends (Fig. 2). The trend analysis indicated that TN10p and TX10p significantly reduced ($P < 0.01$) at the rates of -1.44 days/decade and -0.70 days/decade in the whole China, where 184 stations and 134 stations (92% and 67% of total stations)

exhibited significant decreasing trends, respectively (Table 1). In the four climate zones, TN10p and TX10p also decreased at various magnitudes. The decreasing rates of TN10p (-1.59 days/decade) and TX10p (-0.89 days/decade) were largest in MPZ, but these were smallest in SMZ (-1.27

Table 1 Trends (unit/decade), Mann-Kendall Z, and the number of stations with positive (significant at the 0.05 level) and negative (significant at the 0.05 level) trends in percentile-based and absolute temperature indexes across different climatic zones of China

Climatic zone	Index	1956–2015					1956–1985		1986–2015		Change point (year)
		Trend	Z	Positive	Non-trend	Negative	Trend	Z	Trend	Z	
TCZ	TN10p (days)	-1.35 (-2.18~1.48)	-7**	3 (2)	0	55 (54)	-1.48	-2.5*	-0.72	-3.3**	1988
	TN90p (days)	2.04 (-1.23~5.48)	6.6**	55 (53)	0	3 (3)	0.63	1.4	2.94	3.1**	1987
	TX10p (days)	-0.79 (-1.49~-0.05)	-4.4**	0	0	58 (48)	-0.38	-0.6	-0.65	-1.9	1988
	TX90p (days)	0.99 (-0.38~2.59)	3.9**	52 (48)	1	5 (0)	-0.12	-0.3	1.91	2.2*	1997
	TXx (°C)	0.16 (-0.36~0.71)	2.4*	45 (18)	1	12 (3)	0.05	0.3	0.38	1.8	1997
	TNx (°C)	0.22 (-0.41~1.17)	4.1**	52 (36)	0	6 (1)	-0.02	-0.1	0.38	2.2*	1994
	TXn (°C)	0.40 (-0.06~1.40)	2.9**	55 (25)	1	2 (0)	0.53	1.5	-0.56	-1.4	1982
	TNn (°C)	0.55 (-0.24~1.89)	4.4**	56 (37)	0	2 (0)	0.67	2.5*	-0.47	-1.5	1982
TMZ	TN10p (days)	-1.47 (-2.47~-0.26)	-6.7**	0	0	49 (46)	-1.36	-1.9	-0.75	-2.9**	1988
	TN90p (days)	2.06 (-0.10~4.37)	6.4**	48 (46)	0	1 (0)	0.34	0.6	2.78	3.2**	1988
	TX10p (days)	-0.72 (-1.27~-0.12)	-3.9**	0	0	49 (40)	-0.2	-0.2	-0.43	-1.2	1988
	TX90p (days)	0.68 (-0.21~1.89)	3.3**	42 (26)	3	4 (0)	-0.04	-0.1	1.15	1.5	1994
	TXx (°C)	0.12 (-0.15~0.52)	1.7	33 (13)	3	13 (0)	-0.04	-0.3	0.34	2*	1997
	TNx (°C)	0.18 (-0.12~0.59)	3.5**	45 (27)	0	4 (0)	-0.1	-0.8	0.31	2*	1994
	TXn (°C)	0.35 (0~0.67)	2.6**	48 (20)	0	1 (0)	0.42	1.5	-0.16	-0.7	1988
	TNn (°C)	0.63 (0~1.23)	4.7**	49 (35)	0	0	0.78	2.5*	-0.01	-0.3	1988
MPZ	TN10p (days)	-1.59 (-2.19~0.08)	-7.2**	1 (0)	0	22 (22)	-1.61	-3.1**	-1.23	-3.6**	1987
	TN90p (days)	2.29 (0.44~5.14)	7.2**	23 (22)	0	0	0.89	2.5*	4.07	4.4**	1987
	TX10p (days)	-0.89 (-1.45~-0.50)	-4.6**	0	0	23 (23)	0.18	0.2	-1.51	-3.3**	1998
	TX90p (days)	1.38 (0.73~3.60)	5.5**	23 (23)	0	0	0.28	0.6	2.52	2.9**	1987
	TXx (°C)	0.23 (0~0.39)	3.9**	22 (13)	1	0	0.04	0.4	0.28	1.6	1994
	TNx (°C)	0.27 (0.02~0.51)	5.7**	23 (18)	0	0	-0.05	-0.5	0.43	4.2**	1995
	TXn (°C)	0.36 (-0.05~0.48)	3.6**	21 (10)	0	2 (0)	0.04	0.1	0.85	2.9**	1998
	TNn (°C)	0.58 (-0.03~0.94)	5.7**	22 (17)	0	1 (0)	0.65	2.6**	0.88	3.1**	1990
SMZ	TN10p (days)	-1.27 (-2.45~0.15)	-6.6**	1 (0)	0	69 (62)	-1.05	-2	-1.07	-3**	1989
	TN90p (days)	2.08 (-0.22~7.53)	6.6**	65 (59)	0	5 (0)	0.19	0.5	3.56	4**	1987
	TX10p (days)	-0.36 (-1.82~0.83)	-2.5*	8 (1)	2	60 (23)	0.58	1.6	-0.64	-1.7	1994
	TX90p (days)	1.13 (-0.49~5.29)	4**	63 (41)	0	7 (1)	-1.2	-2.7**	2.94	3.9**	1997
	TXx (°C)	0.10 (-0.13~0.69)	2.6**	53 (19)	3	14 (0)	-0.23	-2.1*	0.28	3**	2002
	TNx (°C)	0.17 (-0.06~0.56)	5.6**	66 (50)	0	4 (0)	0.03	0.2	0.26	3**	1987
	TXn (°C)	0.22 (-0.05~0.48)	3.1**	65 (31)	1	4 (0)	0.02	0.5	0.04	0.6	1992
	TNn (°C)	0.41 (-0.09~0.98)	5.6**	66 (56)	0	4 (0)	0.39	2.5*	0.03	0.1	1985
Whole	TN10p (days)	-1.44 (-2.47~1.48)	-7.7**	5 (2)	0	195 (184)	-1.47	-3.2**	-0.92	-3.2**	1988
	TN90p (days)	2.12 (-1.23~7.53)	7**	191 (180)	0	9 (3)	0.41	1.3	3.21	3.6**	1987
	TX10p (days)	-0.70 (-1.82~0.83)	-5**	8 (1)	2	190 (134)	0.15	0.6	-0.78	-2.6**	1988
	TX90p (days)	1.00 (-0.49~5.29)	4.6**	180 (138)	4	16 (1)	-0.46	-1.5	2.23	2.8**	1994
	TXx (°C)	0.15 (-0.36~0.71)	3.7**	153 (63)	8	39 (3)	-0.03	-0.3	0.30	2.3*	1994
	TNx (°C)	0.22 (-0.41~1.17)	5.2**	186 (131)	0	14 (1)	-0.05	-0.7	0.36	3.2**	1994
	TXn (°C)	0.35 (-0.06~1.40)	4.2**	189 (86)	2	9 (0)	0.30	1.4	0.02	0.1	1988
	TNn (°C)	0.55 (-0.24~1.89)	6.8**	193 (145)	0	7 (0)	0.62	3.7**	0.10	0.3	1981

* and **: Mann-Kendall Z is significant at the 0.05 and 0.01 levels, respectively. *TCZ*: temperate continental zone; *TMZ*: temperate monsoon zone; *MPZ*: mountain plateau zone; *SMZ*: (sub) tropical monsoon zone

and -0.36 days/decade, respectively). Stations with a significantly decreasing trend of TN10p were evenly distributed across the four regions. Only approximately 33% of stations

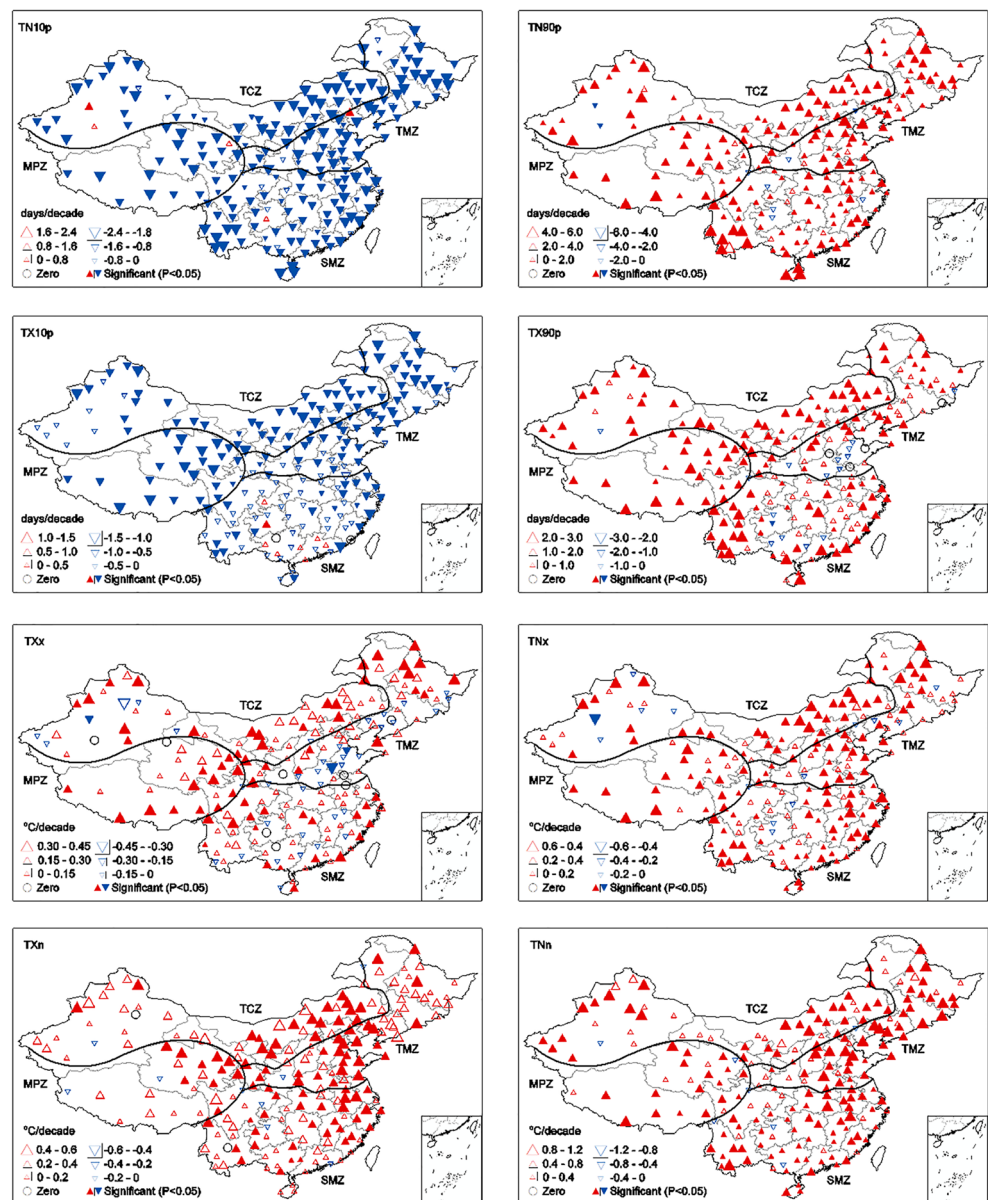
in SMZ showed significant trends for TX10p (Fig. 3). TN90p, TX90p, TXx, TNx, TXn, and TNn increased significantly ($P < 0.01$) at the rates of 2.12 days/decade,

1.00 days/decade, 0.15 °C/decade, 0.22 °C/decade, 0.35 °C/decade, and 0.55 °C/decade over the past 60 years, respectively. The percentages of stations having significantly decreasing trends were 90%, 69%, 31.5%, 65.5%, 43%, and 72.5% in the whole China, respectively. These indexes have also increased in the four climatic zones, showing a similar variation. For TN90p and TX90p, stations in MPZ exhibited the largest change magnitudes (2.29 and 1.38 days/decade), and those in TMZ showed the smallest changes (2.06 and 0.68 days/decade). About 53.1% and 58.6% of stations in TMZ and SMZ increased significantly for TX90p, and 32.7% and 31.4% of stations decreased significantly, respectively. For TXx and TNx, stations with the largest trend magnitudes were distributed in MPZ (0.23 and 0.27 °C/

decade) and those with the smallest magnitudes were distributed in SMZ (0.10 and 0.17 °C/decade). TXn and TNn showed significantly increasing trends ($P < 0.01$) in all four regions, with the lowest rates (0.22 and 0.41 °C/decade) in SMZ. Stations with significantly increasing trends were scattered relatively evenly for the four absolute temperature indexes (Fig. 3).

Although the general trend of percentile-based and absolute temperature indexes was increasing or decreasing during 1956–2015, an abrupt change occurred in the 1980s for most of these indexes according to the Pettitt test, whereas TX90p, TXx, and TNx displayed abrupt changes in the 1990s (Table 1). Comprehensively considering the abrupt changes of the temperature extremes, the studied six decades was separated as two 30-year periods

Fig. 3 Spatial distributions of change trends (per decade) in percentile-based and absolute temperature indexes in China during 1956–2015. Positive/negative trends are shown as up/down triangles, and the filled symbols represent statistically significant trends at the 0.05 level. The size of the triangles is proportional to the magnitude of the trends



(1956–1985 and 1986–2015) to explore their corresponding change trends and rates (Table 1). In the whole China, TX10p underwent a slight increase prior to 1985, but a significant decline after 1985. The trends over the two periods were 0.15 ($P > 0.05$) and -0.78 days/decade ($P < 0.01$), respectively. The change of TX10p was unevenly distributed across China and its decreasing trend was significantly accelerated in MPZ after 1985, while the corresponding trends were not significant in the other zones. TN90p increased insignificantly by 0.41 days/decade ($P > 0.05$) and significantly ($P < 0.01$) by 3.21 days/decade before and after 1985 in the whole China, respectively. Similar trends were also found in contrasting climatic zones. TX90p, TXx, and TNx showed negative trends during 1956–1985 with moderate rates of -0.46 , -0.03 , and -0.05 °C/decade ($P > 0.05$), but significantly positive trends after 1985, with the rates of 2.23, 0.30, and 0.36 °C/decade ($P < 0.05$) in the whole China, respectively. TNn increased significantly ($P < 0.05$) during 1956–1985, but it showed no significant trend ($P > 0.05$) after 1985 in different climatic zones excluding MPZ, where TNn was significantly increased by 0.88 °C/decade during 1985–2015.

3.1.2 Threshold, duration, and other extreme temperature indexes (FD0, ID0, SU25, TR20, CSDI, WSDI, GSL, and DTR)

In the whole China, both frost days (FD0) and ice days (ID0) showed significantly decreasing trends ($P < 0.01$) during 1956–2015, with the average magnitudes of -2.84 and -1.34 days/decade, respectively (Fig. 4). About 81% and 35.5% of the total stations had significantly decreasing trends for FD0 and ID0, respectively. Significantly downward trends ($P < 0.05$) have also been identified in the other three climate zones, with the highest change rates (-3.65 and -2.58 days/decade) in MPZ and the lowest values (-1.66 and -0.11 days/decade) in SMZ. Stations having significantly decreasing trends of FD0 and ID0 represented 58.6% and 15.7% in SMZ, respectively (Table 2; Fig. 5). In the whole China, significant increases in summer days (SU25) and tropical nights (TR20) were observed at 66% and 64% of stations. SU25 and TR20 significantly increased by 1.77 and 1.44 days/decade during 1956–2015 ($P < 0.01$), respectively. Remarkable increases in these two indicators were mainly located in TCZ and SMZ (2.37 and 2.58 days/decade), whereas there were only relatively weak increases in MPZ (0.78 and 0.03 days/decade). All stations located in MPZ showed no statistically significant trend for TR20 during 1956–2015. The stations dominated by significantly negative trends ($P < 0.01$) in cold spell duration indicator (CSDI) and by significantly positive trends ($P < 0.01$) in warm spell duration indicator (WSDI)

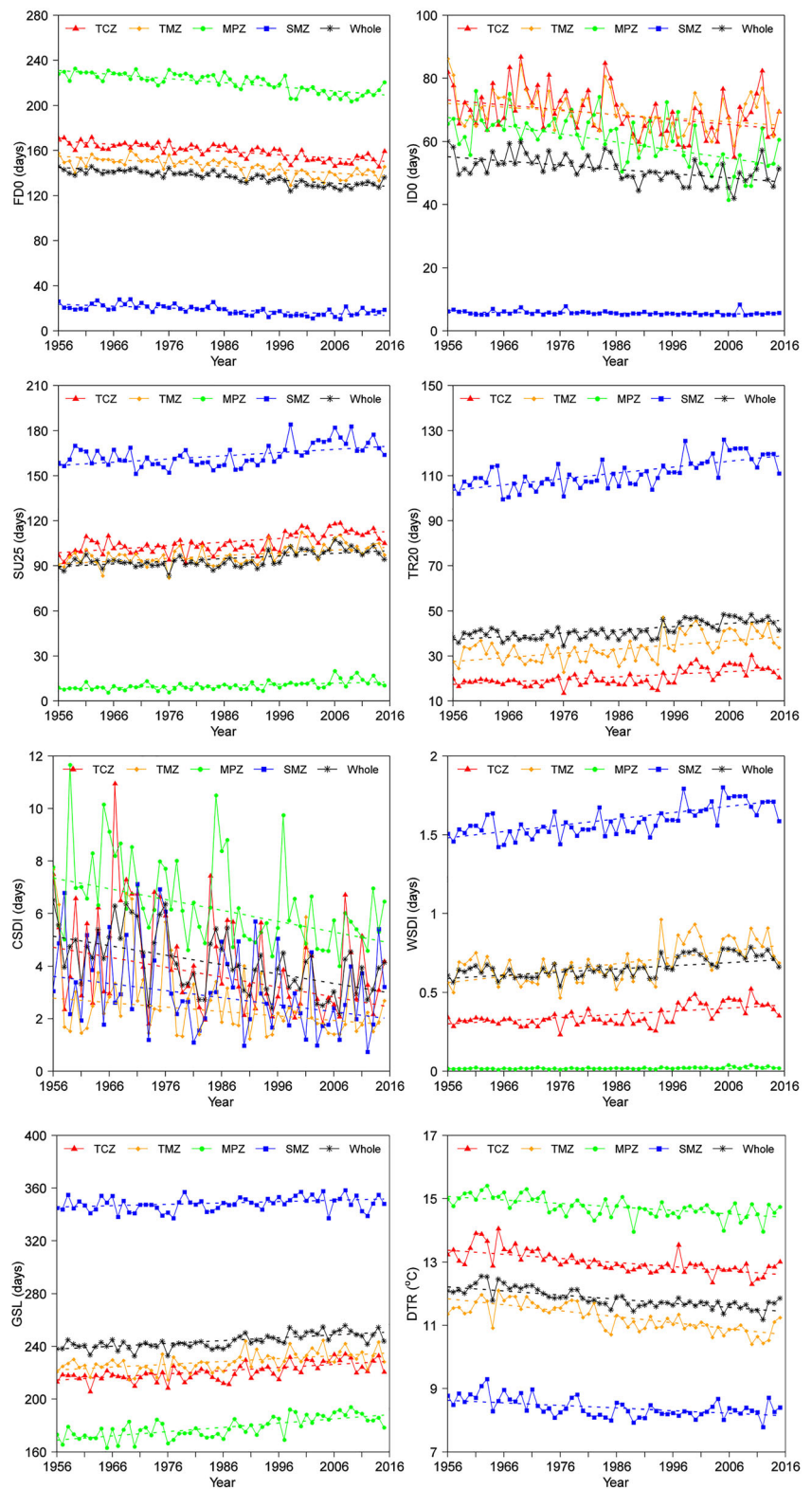
accounted for 14.5% and 64% of the stations, respectively. The regionally averaged change rate of CSDI was the highest in MPZ (-0.41 days/decade) and the lowest in TMZ (-0.17 days/decade). As for WSDI, the regionally averaged trend was very small (0 – 0.04 days/decade) but increasing trends were statistically significant ($P < 0.01$) for all climatic zones except for MPZ (the trends of all stations were not significant). In terms of growing season length (GSL), almost 50% of the stations had increasing trends, with larger trend magnitude in MPZ (3.23 days/decade) and smaller value in SMZ (0.63 days/decade). Significantly negative trends (63.5%) of the diurnal temperature range (DTR) were dominant in the whole China apart from few stations showing significantly positive trends (6.5%). The national trend of DTR was -0.13 °C/decade with significance at the 0.01 level.

Similar to percentile-based and absolute indexes, an abrupt change occurred in the 1980s for FD0, ID0, CSDI, GSL, and DTR according to the Pettitt test. However, change points in SU25, TR20, and WSDI were mainly detected in the 1990s (Table 2). Also, the year of 1985 was considered the dividing line for the trend analysis of threshold and duration indexes. Trends in SU25, TR20, WSDI, and GSL were not significant nationally during 1956–1985 (-0.55 , 0.3, 0.01, and 0.21 days/decade, respectively), while the values were significantly higher than the previous ones after 1985 (3.69, 2.67, 0.04, and 2.72 days/decade, respectively). Similar temporal trends in SU25, TR20, and WSDI were also identified in TCZ, TMZ, and SMZ, which exhibited non-significantly and significantly trends before and after 1985, respectively. Not all the climatic zones showed the same pattern for GSL, which firstly showed decreasing trends before 1985 ($P > 0.05$) and turned to increasing trends after 1985 ($P > 0.05$) in TMZ and SMZ. FD0 exhibited smaller trend magnitude of -1.4 days/decade during 1956–1985 and larger trend magnitude of -3.09 days/decade after 1985 in the whole China. FD0 also presented stronger decreasing trends during 1986–2015 compared with that during 1956–1985 in the four climatic zones. However, the drastically declining trend in DTR mainly occurred during the first 30-year period ($P < 0.05$) except for TMZ. Nationally, DTR decreased rapidly ($P < 0.01$) at a rate of -0.23 °C/decade during 1956–1985 and then declined insignificantly ($P > 0.05$) after 1985 (-0.04 °C/decade).

3.1.3 Comparison of warm and cold extremes

The change rates of warm and cold indexes were further compared and analyzed in Table S1. For warm days (TX90p) versus cool days (TX10p), the national rate of TX90p (1.00 days/decade) was slightly greater than that of TX10p (-0.70 days/decade), with 75% of the stations having greater trend magnitudes in TX90p. However, there was smaller trend magnitude in TX90p than that in

Fig. 4 Annual variations of spatially averaged values of threshold and duration temperature indexes during 1956–2015 across different climatic zones of China



TX10p in TMZ. As for warm nights (TN90p) versus cool nights (TN10p), the national rate in TN90p (2.12 days/decade) was larger compared with that of TN10p (− 1.44 days/decade), among which about 80% of the

stations had greater change rates in TN90p relative to those in TN10p. Similarly, all the climatic zones had greater change rates in TN90p than those in TN10p. Nationally, 77% of the stations showed larger trend

Table 2 Trends (unit/decade), Mann–Kendal Z, and the number of stations with positive (significant at the 0.05 level) and negative (significant at the 0.05 level) trends in threshold and duration temperature indexes across different climatic zones of China

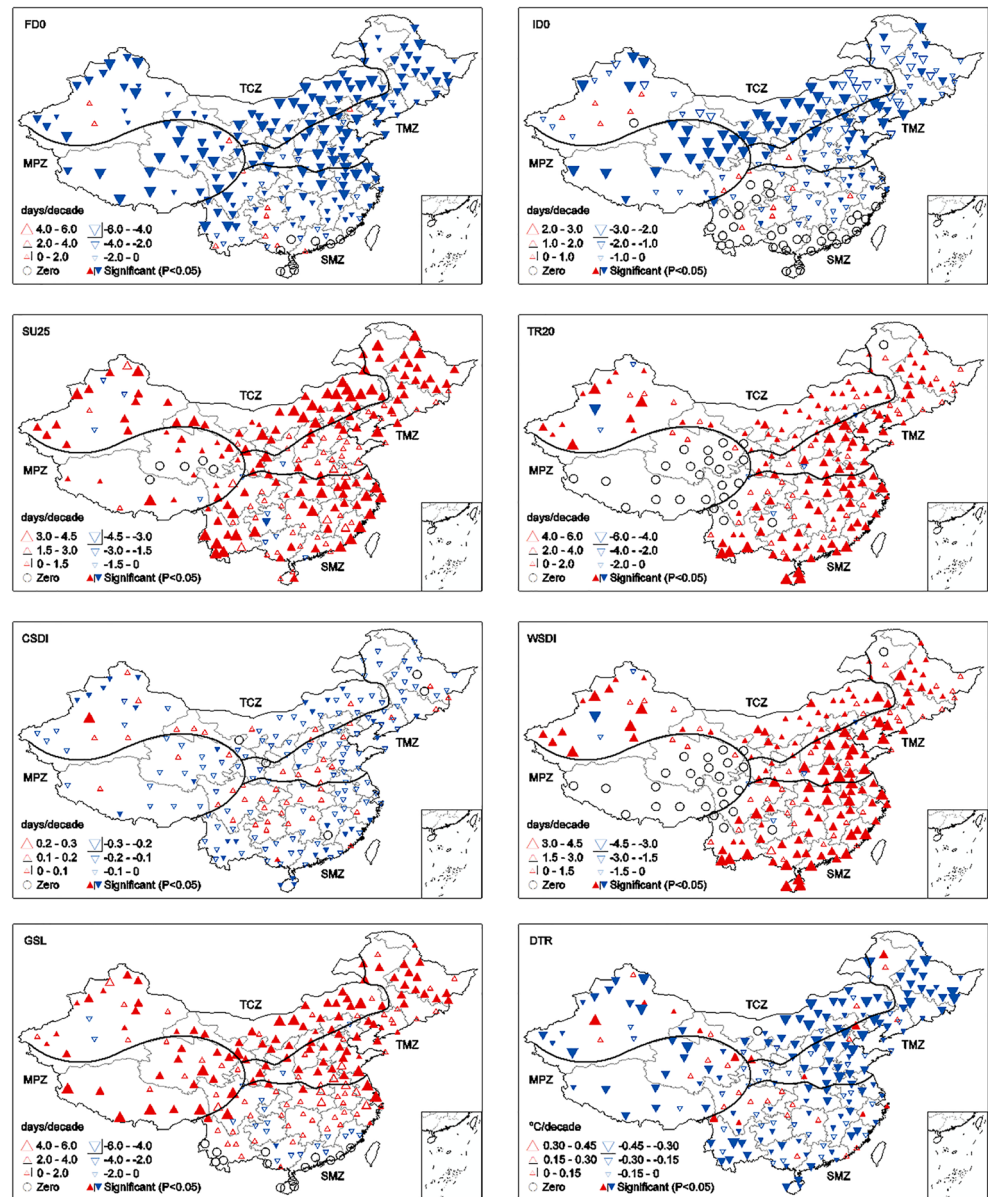
Climatic zone	Index	1956–2015					1956–1985		1986–2015		Change point (year)
		Trend	Z	Positive	Non-trend	Negative	Trend	Z	Trend	Z	
TCZ	FD0 (days)	-3.07 (-6.51~1.18)	-6.7**	3 (0)	0	55 (55)	-2.13	-2.2*	-4.1	-3.3**	1989
	ID0 (days)	-1.55 (-3.72~0.52)	-2.9**	5 (0)	1	52 (27)	-0.17	-0.2	0.83	0.5	1987
	SU25 (days)	2.37 (-1.05~5.13)	4.8**	55 (45)	0	3 (0)	0.63	0.4	4.17	2.9**	1997
	TR20 (days)	1.13 (-4.87~7.50)	4.4**	53 (45)	1	4 (2)	0.02	0	2.68	3.0**	1997
	CSDI (days)	-0.38 (-1.92~1.64)	-0.9	14 (1)	1	43 (10)	-0.32	-0.5	-0.11	-0.7	1989
	WSDI (days)	0.02 (-4.87~7.50)	4.1**	53 (45)	1	4 (2)	0.00	0	0.05	3**	1997
	GSL (days)	2.37 (-0.52~5.00)	5.1**	55 (44)	0	3 (0)	0.77	0.7	4.17	2.8**	1989
	DTR (°C)	-0.13 (-0.50~0.33)	-6**	10 (6)	1	47 (37)	-0.25	-3.6**	-0.04	-0.9	1983
TMZ	FD0 (days)	-3.00 (-5.62~0)	-6.2**	0	0	49 (45)	-1.03	-1.3	-3.76	-2.9**	1989
	ID0 (days)	-1.17 (-2.43~0)	-2.4*	1 (0)	0	48 (22)	-0.32	-0.3	1.59	1.1	1989
	SU25 (days)	1.85 (0~4.23)	4**	48 (31)	0	1 (0)	-0.46	-0.4	3.81	2.8**	1994
	TR20 (days)	1.84 (-1.04~6.18)	4.1**	47 (34)	1	1 (0)	-0.22	-0.3	3.32	2.4*	1994
	CSDI (days)	-0.17 (-1.99~0.73)	-1.2	10 (0)	3	36 (4)	-0.12	-0.6	-0.09	-0.7	1978
	WSDI (days)	0.04 (-1.04~6.18)	4.1**	47 (34)	1	1 (0)	0.00	-0.3	0.07	2.4*	1994
	GSL (days)	2.15 (0~4.60)	4.3**	48 (34)	0	1 (0)	-0.38	-0.4	2.34	1.6	1988
	DTR (°C)	-0.19 (-0.60~0.17)	-6.3**	5 (2)	0	44 (37)	-0.12	-1.5	-0.16	-3.1**	1983
MPZ	FD0 (days)	-3.65 (-7.50~0.67)	-6.7**	1 (0)	0	22 (22)	-1.81	-2.3*	-5.9	-4**	1988
	ID0 (days)	-2.58 (-7.08~0)	-4.5**	2 (0)	0	21 (18)	-0.14	-0.2	-3.44	-2.2*	1987
	SU25 (days)	0.78 (0~3.33)	4.5**	17 (15)	5	1 (0)	0.31	0.9	1.74	3.1**	1994
	TR20 (days)	0.03 (0~0.05)	1.6	0	20	3(0)	0.01	0.5	0.08	1.0	1994
	CSDI (days)	-0.41 (-0.92~0.17)	-1.6	5 (0)	0	18 (3)	-0.54	-1.6	-0.20	-0.8	1988
	WSDI (days)	0.00 (0~0)	0	0	20	3 (0)	0.00	0	0.00	0	1994
	GSL (days)	3.23 (0.57~9.29)	5.5**	23 (15)	0	0	0.76	0.8	4.19	3**	1988
	DTR (°C)	-0.11 (-0.37~0.25)	-4.7**	6 (1)	0	17 (14)	-0.20	-3.1**	-0.07	-1.2	1974
SMZ	FD0 (days)	-1.66 (-5.93~0)	-5.1**	7 (0)	9	54 (41)	-0.46	-0.8	0.03	0.1	1987
	ID0 (days)	-0.11 (-2.31~0)	-0.7	6 (0)	34	30 (11)	-0.03	-0.3	-0.02	-0.3	1987
	SU25 (days)	2.14 (-2.33~9.06)	3.7**	64 (41)	0	6 (1)	-1.93	-1.8	5.78	3.8**	1994
	TR20 (days)	2.58 (0~11.43)	5.7**	64 (49)	4	2 (0)	0.88	1.1	4.95	3.9**	1994
	CSDI (days)	-0.27 (-3.18~1.64)	-1.6	19 (1)	1	50 (12)	-0.49	-1.4	-0.44	-1.2	1978
	WSDI (days)	0.04 (0~11.43)	5.7**	64 (49)	4	2 (0)	0.01	1.1	0.07	3.9**	1994
	GSL (days)	0.63 (-0.36~7.85)	1.2	39 (7)	14	17 (1)	-0.68	-0.3	0.85	0.7	1989
	DTR (°C)	-0.08 (-0.44~0.26)	-3.7**	13 (4)	0	57 (39)	-0.25	-3.7**	0.01	0.3	1980
Whole	FD0 (days)	-2.84 (-7.50~1.18)	-7.3**	11 (0)	9	180 (163)	-1.4	-2.4*	-3.09	-3**	1987
	ID0 (days)	-1.34 (-7.08~0.52)	-4.4**	14 (0)	35	151 (78)	-0.13	-0.7	0.03	0.1	1987
	SU25 (days)	1.77 (-2.33~9.06)	4.4**	184 (132)	5	11 (1)	-0.55	-0.8	3.69	3.1**	1994
	TR20 (days)	1.44 (-4.87~11.43)	5.2**	167 (128)	26	7 (2)	0.30	0.7	2.67	3.2**	1994
	CSDI (days)	-0.36 (-3.18~1.64)	-1.8	48 (2)	5	147 (29)	-0.42	-1.6	-0.20	-1.1	1978
	WSDI (days)	0.02 (-4.87~11.43)	5.0**	167 (128)	26	7 (2)	0.01	0.4	0.04	3.1**	1994
	GSL (days)	2.16 (-0.52~9.29)	5.7**	165 (100)	14	21 (1)	0.21	0.3	2.72	2.5*	1988
	DTR (°C)	-0.13 (-0.60~0.33)	-6.5**	34 (13)	1	165 (127)	-0.23	-3.7**	-0.04	-1.2	1981

* and **: Mann-Kendall Z is significant at the 0.05 and 0.01 levels, respectively. *TCZ*: temperate continental zone; *TMZ*: temperate monsoon zone; *MPZ*: mountain plateau zone; *SMZ*: (sub) tropical monsoon zone

magnitudes in minimum T_{\max} (TXn), and the national magnitude in TXn was 0.35 °C/decade, which was 2.3 times larger relative to that of maximum T_{\max} (TXx)

(0.15 °C/decade). Minimum T_{\min} (TNn) (0.55 °C/decade) was 2.5 times greater than that of maximum T_{\min} (TNx) (0.22 °C/decade), with 85% of the stations having greater

Fig. 5 Spatial distributions of change trends (per decade) in threshold and duration temperature indexes in China during 1956–2015. Positive/negative trends are shown as up/down triangles, and the filled symbols represent statistically significant trends at the 0.05 level. The size of the triangles is proportional to the magnitude of the trends



trend magnitudes in TNn. The trends of TNx showed greater change rates than those of TXx at 59% of the stations, and 76% of the stations showed larger magnitudes in TNn than those in TXn. Frost days (FD0) (−2.84 days/decade) exhibited greater national change rate than summer days (SU25) (1.77 days/decade) and tropical days (TR20) (1.44 days/decade), with 64% and 70% of the stations having larger trend magnitudes in FD0, respectively. FD0 showed larger trend magnitudes than those of growing season length (GSL) (−2.84 and 2.16 days/decade, respectively) at 72% of the stations. About 83%, 87%, and 57% of the stations had greater trend magnitudes of ice days (ID0) than those in SU25, TR20, and GSL in SMZ, respectively. Further, changes of temperature extremes on the basis of daily minimum

temperature (TN10p, TN90p, TNx, and TNn) appeared to have larger changes than those based on daily maximum temperature (TX10p, TX90p, TXx, and TXn) both nationally and regionally.

3.1.4 Correlation coefficients of extreme temperature indexes

To explore if the extreme temperature indexes selected here were indicative to the mean air temperature (T_{mean}) and clarify their interactions and relationships among the 16 indexes, the Pearson correlation coefficient was determined for the four climatic zones (Table S2). Nationally, all the indexes had high correlations with T_{mean} , having correlation coefficient greater than 0.5 ($P < 0.01$). Regionally, compared with the other indexes, DTR had slightly lower correlations with T_{mean} , and

even failed the significance test in SMZ ($P > 0.05$). Overall, positive correlations were significant ($P < 0.01$) between T_{mean} and warm extremes, and the largest values of correlation coefficient were higher than 0.90 for TN90p across different climatic zones. A comparison of various cold indexes revealed that TN10p and FD0 had stronger negative correlations with T_{mean} , with the coefficients of approximately 0.90 except for SMZ. For warm extremes, there were high positive correlations among warm indexes, with the highest correlation coefficient existing between TR20 and WSDI (nearly 1). In addition, cold indexes versus cold indexes also showed significant positive correlations except for the two absolute indexes of TXn and TNn. The highest coefficient among cold indexes existed between TXn and TNn ($R > 0.85$), while the highest value of 0.77 existed between TN10p and FD0 in SMZ. The four absolute indexes (TXn, TNn, TXx, and TNx) had a positive correlation, where the highest correlation coefficient was found between TNx and TXx, indicating that the absolute indexes exhibited similar variations over time. However, the correlation coefficients between the absolute indexes and most other indexes failed the significance test ($P < 0.05$) in TCZ and TMZ. Cold indexes (TX10p, TN10p, FD0, ID0, and CSDI) versus all warm indexes showed negative correlations, confirming that these two categories of indexes showed exact opposite change trends over the past 60 years. For TMZ and SMZ, ID0 versus most warm indexes showed no significant negative correlation ($P > 0.05$). The correlations between CSDI and warm indexes (SU25, TR20, and WSDI) were not significant in MPZ.

3.2 Spatiotemporal changes of extreme precipitation indexes

3.2.1 Percentile-based and absolute extreme precipitation indexes (R95P, R99p, RX1day, and RX5day)

Relative to temperature extremes, changes of precipitation extremes over the span of 1956–2015 showed lower significance (Fig. 6, Table 3). Nationally, the very wet day precipitation (R95p) and extremely wet day precipitation (R99p) increased insignificantly during 1956–2015 ($P > 0.05$), with the values of 2.71 and 1.51 mm/decade, respectively. Stations with positive trends in these two indexes represented 63.0% and 57.5%, in which only 9.5% and 9.6% of the stations were featured by significantly increasing trends ($P < 0.05$), mostly located in SMZ. Stations having positive trends in TCZ and TMZ occupied 62.1% and 38.8% in R95p and 53.4% and 36.7% in R99p, respectively. In general, non-significantly downward trends were detected for R95p and R99p in TCZ and TMZ during 1956–2015 ($P > 0.05$) (Fig. 7). For the absolute indexes of maximum 1-day (RX1day) and 5-day (RX5day) precipitation, more stations showed upward trends compared with those having downward trends in the whole

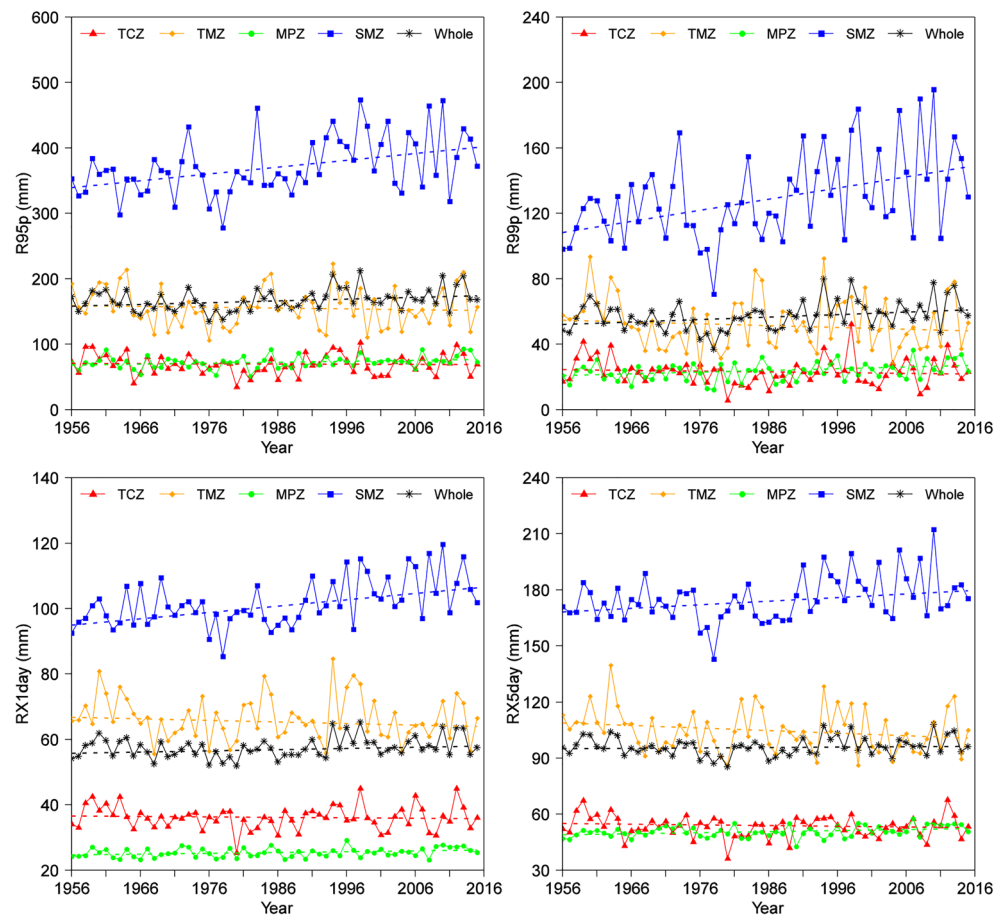
China (61% versus 37.5%, 56% versus 44%, respectively), although the amount of stations experiencing significantly positive trends were generally small ($P < 0.05$) (8.5% and 8% of total stations, respectively). The spatially averaged values of RX1day and RX5day non-significantly increased by 0.37 and 0.22 mm/decade over the past six decades ($P > 0.05$), respectively. The regional trends in these two indexes across different climatic zones were not consistent. RX1day and RX5day showed insignificantly negative trends ($P > 0.05$) in TCZ, TMZ, and MPZ, while they showed significantly positive trends ($P < 0.05$) in SMZ during 1956–2015. The largest increasing rates of R95P, R99p, RX1day, and RX5day occurred in SMZ (10.45, 6.82, 1.94, and 1.93 mm/decade, respectively).

There were abrupt changes in the variations of percentile-based and absolute precipitation extremes in the 1970s in TCZ and TMZ, while the abrupt change years were identified in the 1990s in MPZ and SMZ. Comprehensively considering the abrupt changes of these precipitation extremes, the change trends between the two 30-year periods of 1956–1985 and 1986–2015 were further analyzed and compared. Weak decreases in R95P, R99p, RX1day, and RX5day before 1985 changed to insignificant increases from 1986 to 2015 in the whole China. The change trends in R95P, R99p, RX1day, and RX5day during the two periods were completely opposite in TCZ. R95P, R99p, and RX1day showed significantly downward trends ($P < 0.05$) at rates of -7.06 , -3.41 , and -1.27 mm/decade during 1956–1985, but non-significantly upward trends were detected during 1986–2015 ($P > 0.05$) in TCZ. The decreasing trends were not significant ($P > 0.05$) during 1956–1985 and the change trends remained stable after 1985 in TMZ. Increasing trends were detected for all the four precipitation indexes in MPZ during the whole period, but the upward trends were accelerated during 1986–2015 compared with the period of 1956–1985, and the upward trends in R95P, RX1day, and RX5day passed the significant tests. Regionally averaged values of R95P, R99p, RX1day, and RX5day were larger after 1985 in SMZ (11.81, 9.01, 3.91, and 3.61 mm/decade, respectively).

3.2.2 Threshold and duration extreme precipitation indexes (R10mm, R25mm, R50mm, CDD, and CWD)

Spatially averaged heavy precipitation days (R10mm), extremely heavy precipitation days (R25mm), and rainstorm days (R50mm) exhibited increasing trends from 1956 to 2015 in the whole China, with the values of 0.06, 0.02, and 0.02 days/decade, respectively, in which 90, 98, and 110 stations (45%, 49%, and 55% of total stations) displayed increasing trends. However, only 14, 13, and 11 stations exhibited significantly upward trends ($P < 0.05$) (Table 4, Fig. 8). The changes of R10mm in TCZ, TMZ, and SMZ showed mixed patterns of upward and downward trends, 53.4% upward

Fig. 6 Annual variations of spatially averaged values of percentile-based and absolute precipitation indexes during 1956–2015 across different climatic zones of China



versus 43.1% downward in TCZ, 30.6% versus 63.3% in TMZ and 35.7% versus 58.6% in SMZ. MPZ was dominated by positive trends in R10mm (82.6%) apart from some stations having negative trends (17.4%). The regionally averaged trend in R10mm was 0.63 days/decade ($P < 0.01$). The stations having larger increasing trends in R25mm (0.6–0.9 days/decade) and R50mm (0.4–0.6 days/decade) were mainly located in SMZ. These two indexes were enhanced significantly over the past 60 years in SMZ (0.20 and 0.12 days/decade, respectively). Stations remained unchanged in R50mm occupied 74% in MPZ, and the majority of the stations exhibited no upward or downward trend in the western part of TCZ (Fig. 9). Nationally, consecutive wet days (CWD) significantly ($P < 0.05$) decreased during 1956–2015 (-0.05 days/decade), although significantly downward trends were only detected at 18 stations, in which 12 stations were located in SMZ. More stations showed upward trends in MPZ compared with those having downward trends, and CWD showed an increasing trend in this region. CWD decreased at a rate of -0.06 days/decade in TMZ ($P > 0.05$) and -0.14 days/decade in SMZ ($P < 0.05$). Consecutive dry days (CDD) decreased during 1956–2015 ($P > 0.05$) in the whole China, although most stations in TMZ and SMZ presented positive trends. The

spatial distribution of change trends in CDD was opposite to that of CWD. CDD remained stable in TMZ but it showed an increasing trend in SMZ. CDD decreased at rates of -1.08 ($P > 0.05$) and -1.69 ($P < 0.05$) in TCZ and MPZ, respectively.

The Pettitt test showed that the abrupt change points in threshold and duration indexes were mainly detected from the 1970s to the 1990s, and the general trends of these indexes in different climatic zones as well as the whole China during the two periods 1956–1985 and 1986–2015 are shown in Table 4. R10mm, R25mm, and R50mm firstly showed decreasing trends during 1956–1985 ($P > 0.05$) and shifted to increase after 1985 ($P > 0.05$) in the whole China. The same trends in these three indexes were also identified in TCZ and TMZ. R10mm and R25mm presented greater increasing trends from 1986 to 2015 than those during the whole period in MPZ. The regional upward trends in CDD were identified in all the four climatic zones during 1956–1985, but the trends were mixed from 1986 to 2015, with downward trends in TCZ, TMZ, and MPZ and upward trends in SMZ. There were no obvious changes in CWD except for SMZ. CWD showed a positive trend during 1956–1985 with a gentle rate of -0.07 days/decade ($P > 0.05$), but a significantly positive trend (-0.29 days/decade) was identified after 1985 in SMZ.

Table 3 Trends (unit/decade), Mann–Kendal Z, and the number of stations with positive (significant at the 0.05 level) and negative (significant at the 0.05 level) trends in percentile-based and absolute precipitation indexes across different climatic zones of China

Climatic zone	Index	1956–2015				1956–1985		1986–2015		Change point (year)	
		Trend	Z	Positive	Non-trend	Negative	Trend	Z	Trend		Z
TCZ	R95p (mm)	-0.28 (-11.46~13.25)	-0.1	36 (3)	1	21 (1)	-7.06	-2.1*	2.16	0.6	1975
	R99p (mm)	-0.45 (0~0.59)	-0.8	31 (3)	5	22 (2)	-3.41	-2.4*	1.57	0.9	1980
	RX1day (mm)	-0.14 (-2.58~3.89)	-0.5	34 (4)	0	24 (1)	-1.27	-2.0*	0.10	0.1	1975
	RX5day (mm)	-0.37 (-5.6~4.13)	-0.8	32 (8)	0	26 (3)	-2.05	-1.7	0.07	0.1	1975
TMZ	R95p (mm)	-1.27 (-18.22~8.97)	-0.5	19 (0)	2	28 (1)	-5.72	-0.6	0.11	0	1975
	R99p (mm)	-1.11 (0~0)	-0.8	18 (1)	2	29 (0)	-6.12	-1.3	0.20	0.1	1976
	RX1day (mm)	-0.48 (-4.67~4.33)	-0.9	20 (0)	0	29 (2)	-1.01	-0.5	-0.15	-0.1	1978
	RX5day (mm)	-1.38 (-9.44~7.49)	-1.6	17 (0)	0	32 (1)	-2.76	-1.2	0.26	0.2	1977
MPZ	R95p (mm)	1.47 (-4.71~9.65)	1.9	17 (3)	0	6 (0)	0.15	0.3	3.40	2.6*	1993
	R99p (mm)	1.04 (0~1.68)	1.8	14 (2)	0	9 (0)	0.75	0.4	2.73	1.9	1991
	RX1day (mm)	0.25 (-0.4~1.18)	0.6	13 (2)	2	8 (0)	0.28	1.0	0.66	2.5*	1996
	RX5day (mm)	0.56 (-0.71~2.47)	0.9	17 (1)	0	6 (0)	0.29	0.8	1.53	2.4*	1999
SMZ	R95p (mm)	10.45 (-31.85~44.31)	3.1**	54 (6)	0	16 (2)	-0.36	-0.1	11.81	3.0**	1991
	R99p (mm)	6.82 (-5.55~35.08)	3.4**	52 (5)	4	14 (1)	0.80	0.2	9.01	2.6*	1989
	RX1day (mm)	1.94 (-7.31~13.95)	4**	55 (8)	1	14 (2)	0.32	0.3	3.91	2.7**	1990
	RX5day (mm)	1.93 (-12.53~16.81)	2.4*	46 (7)	0	24 (3)	-1.68	-0.8	3.61	1.5	1990
Whole	R95p (mm)	2.71 (-31.85~44.31)	1.7	126 (12)	3	71 (4)	-3.03	-0.6	3.92	1.0	1990
	R99p (mm)	1.51 (-5.55~35.08)	1.5	115 (11)	11	74 (3)	-1.50	-0.9	2.72	1.4	1989
	RX1day (mm)	0.37 (-7.31~13.95)	1.7	122 (17)	3	75 (5)	-0.54	-0.7	0.92	1.7	1994
	RX5day (mm)	0.22 (-12.53~16.81)	0.6	112 (16)	0	88 (7)	-1.64	-1.5	1.73	1.5	1994

* and **: Mann-Kendall Z is significant at the 0.05 and 0.01 levels, respectively. *TCZ*: temperate continental zone; *TMZ*: temperate monsoon zone; *MPZ*: mountain plateau zone; *SMZ*: (sub) tropical monsoon zone

3.2.3 Other extreme precipitation indexes (PRCPTOT and SDII)

Nationally averaged annual total precipitation (PRCPTOT) showed a statistically non-significant trend during 1956–2015 in the whole China. PRCPTOT underwent a slight decrease during 1956–1985, but it was increased by 6.44 mm/decade ($P > 0.05$) after 1985. Stations having increasing trends were mainly situated in western and southeastern China. A significant increasing trend was detected over the past 60 years in MPZ (7.58 mm/decade, $P < 0.01$), with a sharp increase during 1986–2015 (13.44 mm/decade). Stations having larger increasing (30–45 days/decade) and decreasing (-45~ -30 days/decade) trends in PRCPTOT were located in SMZ, and the averaged magnitude was 7.08 days/decade ($P > 0.05$). PRCPTOT showed negative trends during 1956–1985 at the rates of -10.97 in TCZ and -17.52 mm/decade in TMZ ($P > 0.05$), but it showed positive trends after 1985 at the rates of 4.00 and 4.89 mm/decade ($P > 0.05$), respectively. Daily rainfall intensity (SDII) was significantly ($P < 0.01$) increased in MPZ during 1956–2015 (0.10 mm/day/decade), with a sharp increase from 1986 to 2015 (0.26 mm/day/decade). The regionally averaged

SDII in the other climatic zones (TCZ, TMZ, and SMZ) showed weak decreases during 1956–1985, but underwent positive trends after 1985.

3.2.4 Correlation coefficient of extreme precipitation indexes

The correlation coefficients of the extreme precipitation indexes are presented in Table S3. Nationally, all the indexes apart from consecutive dry days (CDD) ($R = -0.35$) and consecutive wet days (CWD) ($R = 0.26$) showed great correlations with annual total precipitation (PRCPTOT) ($P < 0.05$). Compared with other indexes, CDD and CWD also showed slightly lower correlations with PRCPTOT in TMZ, MPZ, and SMZ and even failed the significance test for CDD in these regions ($P > 0.05$). However, PRCPTOT was well related with all extreme precipitation indexes in TCZ, with correlation coefficients larger than 0.50 ($P < 0.01$). The maximum value of correlation coefficients between PRCPTOT and precipitation extremes was higher than 0.97 for heavy precipitation days (R10mm) across different climatic zones. Besides, significant statistical correlations existed in these extreme precipitation indexes, excluding CDD and CWD. The highest correlation coefficient in these extreme precipitation indexes existed

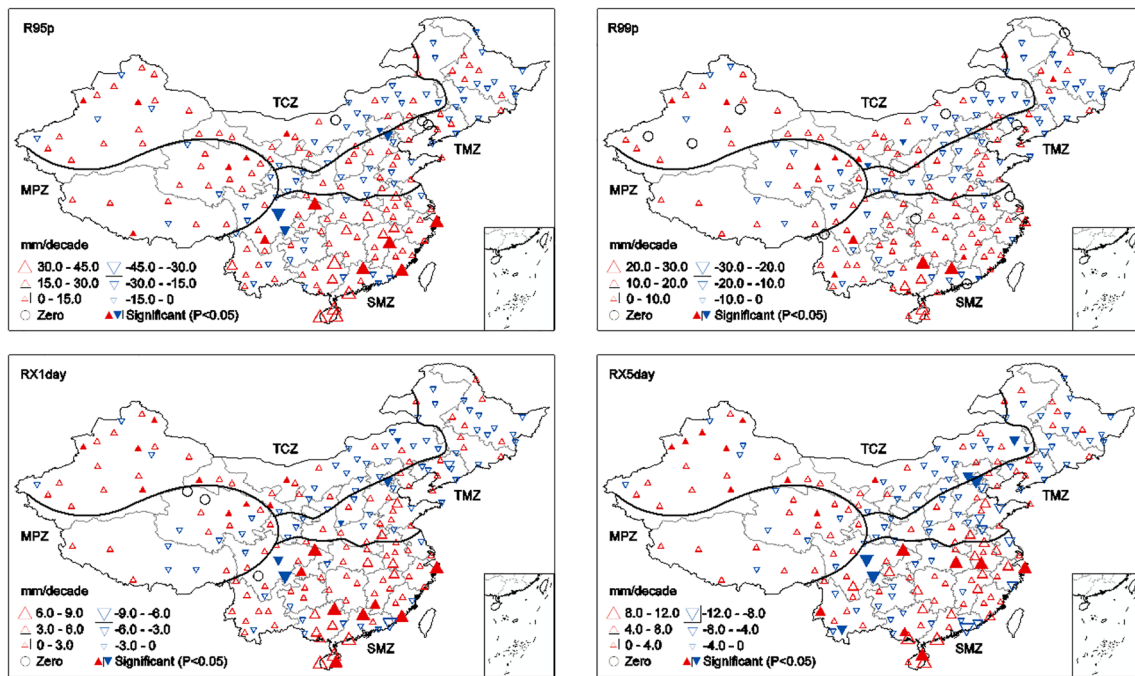


Fig. 7 Spatial distributions of change trends (per decade) in percentile-based and absolute precipitation indexes in China during 1956–2015. Positive/negative trends are shown as up/down triangles, and the filled

symbols represent statistically significant trends at the 0.05 level. The size of the triangles is proportional to the magnitude of the trends

between R10mm and R25mm in TCZ and TMZ ($R = 0.91$ and 0.93 , respectively), while the highest values were identified between R99 and R50mm in SMZ and the whole China ($R = 0.95$ and 0.94 , respectively).

4 Discussion

4.1 Changes of temperature and precipitation extremes in the whole China during 1956–2015

The present results suggested that the trends of temperature extremes in the whole China generally agreed with previous studies, with a general warming trend during the past six decades (Choi et al. 2009; Ruml et al. 2017). However, changes of cool/warm nights (TN10p/TN90p) were more prominent than those of cool/warm days (TX10p/TX90p) in the whole China during 1956–2015. Faster increases were observed for maximum and minimum T_{\min} (TNx, TNn) than maximum and minimum T_{\max} (TXx, TXn). These indicated that the trends in T_{\min} -related extremes (night extremes) were faster than those of T_{\max} -related extremes (day extremes), and highlighting the greater nighttime warming relative to the daytime warming (Zhou et al. 2016; Shi et al. 2018). This asymmetry resulted in a national decreasing trend in DTR over the past 60 years. Cold extremes, such as TNn, TXn, and FD0, appeared to be warming faster than warm extremes (TNx, TXx, SU25, TR20), which are in agreement with the more quickly warming in winter temperatures (IPCC 2007). In the present

study, only SDII exhibited a significantly increasing trend during 1956–2015, whereas the other ten extreme precipitation indexes exhibited no significant trends in the whole China. This is generally good consistent with the results of Choi et al. (2009) and Shi et al. (2018), who revealed that there was a much lower level of statistical significance in precipitation extremes compared with temperature extremes.

An abrupt change in climate is a usual and vital phenomenon in nature. Our results revealed that cold indexes presented abrupt changes in the 1980s, but warm indexes altered suddenly in the 1990s (Table 1 and 2). For extreme precipitation indexes, the abrupt changes in TCZ and TMZ (1970s) were earlier than those in MPZ and SMZ as well as the whole China (1990s) (Tables 3 and 4). Considerable exploratory studies have explored the mechanisms responsible for these differences, such as atmospheric circulation oscillations (Liu et al. 2019), rapid urbanization and dramatic economic growth (Lu et al. 2016; Li et al. 2017), volcanic eruption (Guo and Liu 2002), and nuclear explosion (Voitsekhovich et al. 2007); but opinions varied on this aspect. This can be connected with various weather conditions, topography, and other factors affecting regional climate. However, the reasons of abrupt climate change are not yet clear and further analysis is needed in the future. Obviously, the changes of extreme temperature indexes were different between 1956–1985 and 1986–2015. During 1956–1985, the trend of temperature indexes was more ambiguous, and several indexes like TX10p, TX90p, TXx, TNx, and SU25 showed cooling trends in the whole China. However, these indexes started to show warming

Table 4 Trends (unit/decade), Mann–Kendal Z, and the number of stations with positive (significant at the 0.05 level) and negative (significant at the 0.05 level) trends in threshold, duration, and other precipitation indexes across different climatic zones of China

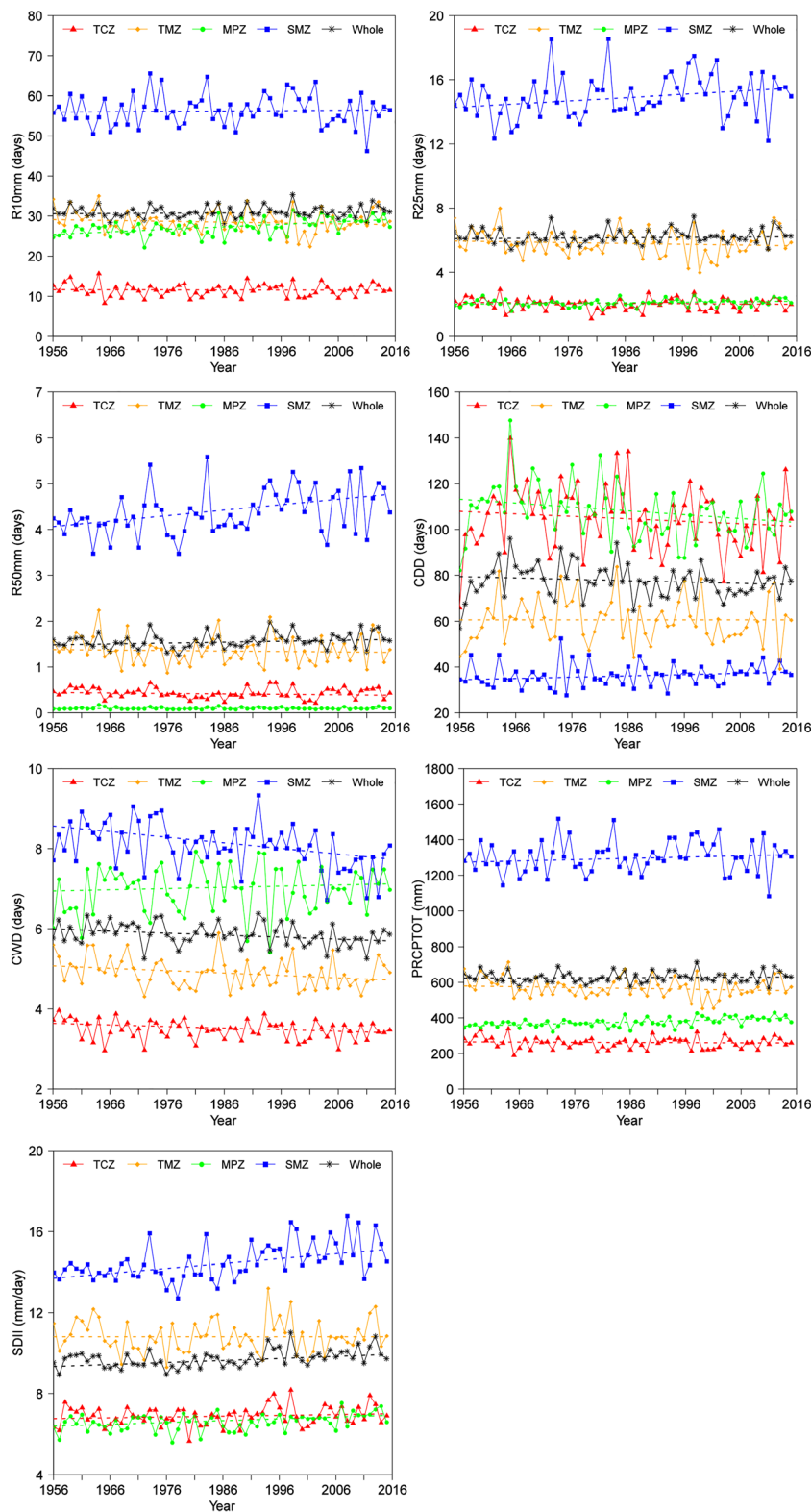
Climatic zone	Index	1956–2015					1956–1985		1986–2015		Change point (year)
		Trend	Z	Positive	Non-trend	Negative	Trend	Z	Trend	Z	
TCZ	R10mm (days)	-0.02 (-0.67~0.75)	-0.1	31 (6)	2	25 (1)	-0.38	-1.0	0.15	0.5	1975
	R25mm (days)	-0.02 (-0.3~0)	-0.7	31 (5)	5	22 (2)	-0.15	-1.6	0.03	0.4	1975
	R50mm (days)	-0.01 (-0.30~0.01)	-0.8	25 (4)	21	12 (2)	-0.05	-2.9**	0.02	0.9	1980
	CDD (days)	-1.08 (-12.86~7)	-0.9	28 (2)	1	29 (3)	4.65	1.4	-1.08	-0.2	1987
	CWD (days)	-0.04 (-0.23~0)	-1.9	22 (3)	3	33 (3)	-0.09	-1.6	-0.02	-0.3	1980
	PRCPTOT (mm)	-1.07 (-17.21~17.27)	-0.5	30 (8)	0	28 (1)	-10.97	-1.6	4.0	0.6	1975
	SDII (mm/day)	0.04 (-0.21~0.33)	1.1	41 (5)	2	15 (1)	-0.05	-0.5	0.1	0.7	1990
TMZ	R10mm (days)	-0.21 (-0.74~0.27)	-0.9	15 (0)	3	31 (1)	-0.86	-1.2	0.35	0.5	1975
	R25mm (days)	-0.05 (-0.25~0)	-0.6	12 (0)	5	32 (0)	-0.20	-1.1	0.17	0.6	1975
	R50mm (days)	-0.01 (-0.05~0)	-0.3	24 (1)	3	22 (1)	-0.04	-0.7	0.07	1.0	1975
	CDD (days)	0.00 (-6.22~3.33)	0	29 (1)	3	17 (3)	3.58	1.8	-0.13	-0.2	1971
	CWD (days)	-0.06 (-0.24~0)	-1.9	14 (0)	3	32 (3)	-0.18	-1.7	0.01	0.1	1973
	PRCPTOT (mm)	-4.5 (-23.64~6.13)	-1.1	10 (0)	0	39 (1)	-17.52	-1.2	4.89	0.6	1975
	SDII (mm/day)	0.00 (-0.19~0.29)	0	29 (0)	4	16 (0)	-0.06	-0.4	0.11	0.6	1975
MPZ	R10mm (days)	0.63 (-0.2~0.77)	4.1**	19 (5)	0	4 (0)	0.45	1.1	0.94	2.4*	1998
	R25mm (days)	0.03 (0~0.50)	1.9	13 (3)	1	9 (0)	-0.01	-0.4	0.07	1.7	1989
	R50mm (days)	0.00 (0~0)	0	4 (0)	17	2 (0)	0.00	0	0.00	0	1989
	CDD (days)	-1.69 (-10.35~1.61)	-2.0*	5 (0)	3	15 (2)	1.21	0.6	-2.55	-2.0*	1986
	CWD (days)	0.03 (-0.09~0.33)	0.6	14 (3)	1	8 (0)	0.15	1.2	0	0	1974
	PRCPTOT (mm)	7.58 (-0.51~16.44)	4.0**	22 (7)	0	1 (0)	4.98	1.0	13.44	2.4*	1998
	SDII (mm/day)	0.09 (-0.06~0.25)	2.7**	20 (3)	0	3 (0)	0.12	1.1	0.26	3.4**	1993
SMZ	R10mm (days)	0.09 (-1.3~1.67)	0.3	25 (3)	4	41 (3)	0.73	0.7	-0.22	-0.2	2003
	R25mm (days)	0.20 (-0.61~1.29)	2.0*	42 (5)	4	24 (2)	0.16	0.7	0.25	0.7	1993
	R50mm (days)	0.12 (-0.24~0.52)	2.8**	57 (6)	4	9 (1)	0.03	0.4	0.16	1.2	1991
	CDD (days)	0.56 (-1.54~3.68)	1.8	46 (4)	2	22 (0)	0.02	0.1	0.64	1.0	2004
	CWD (days)	-0.14 (-0.59~0.18)	-3.1**	18 (0)	3	49 (12)	-0.07	-0.7	-0.29	-2.6**	1999
	PRCPTOT (mm)	7.08 (-58.42~70.22)	1.1	38 (4)	0	32 (3)	9.26	0.7	8.09	0.5	1993
	SDII (mm/day)	0.24 (-0.39~0.72)	4.0**	58 (14)	2	10 (1)	-0.11	-1.1	0.36	1.9	1991
Whole	R10mm (days)	0.06 (-1.3~1.67)	0.6	90 (14)	9	101 (5)	-0.10	-0.4	0.31	0.7	1990
	R25mm (days)	0.02 (-0.61~1.29)	0.8	98 (13)	15	87 (4)	-0.03	-0.2	0.06	0.6	1993
	R50mm (days)	0.02 (-0.24~0.52)	1.8	110 (11)	45	45 (4)	-0.01	-0.2	0.05	1.5	1991
	CDD (days)	-0.6 (-12.86~7)	-1.1	108 (7)	9	83 (8)	2.82	1.3	0.78	0.4	1987
	CWD (days)	-0.05 (-0.59~0.33)	-1.5	68 (6)	10	122 (18)	-0.02	-0.5	-0.06	-1.0	1997
	PRCPTOT (mm)	0.91 (-58.42~70.22)	0.4	100 (19)	0	100 (5)	-3.4	-0.4	6.44	0.5	1990
	SDII (mm/day)	0.10 (-0.39~0.72)	3.1**	148 (22)	8	44 (2)	-0.03	-0.6	0.22	2.4*	1994

* and **: Mann-Kendall Z is significant at the 0.05 and 0.01 levels, respectively. *TCZ*: temperate continental zone; *TMZ*: temperate monsoon zone; *MPZ*: mountain plateau zone; *SMZ*: (sub) tropical monsoon zone

trends after 1985. It is noteworthy that the warming trends in TX90p, TXx, SU25, and WSDI during 1986–2015 doubled the changes over the whole period. This confirmed that there was an accelerated warming after the mid-1980s, which was in accordance with the findings in the Yangtze River Basin (Guan et al. 2015) and in northeastern China (Yu and Li 2015). Besides, it is worth noting that the increment of TNn was large ($P < 0.01$) during 1956–1985 while the increment was smaller

after 1985, which resulted in a small decreasing trend in DTR from 1986 to 2015. This corroborated the finding of Liu et al. (2004), who indicated that the decrease in DTR halted since 1990 because T_{\max} and T_{\min} grew at a similar rate during the 1990s. Time-series analyses revealed that most extreme precipitation indexes exhibited an upward trend after 1985 in different climatic zones, although a drying tendency was observed in TCZ and TMZ during 1956–1985. However, the

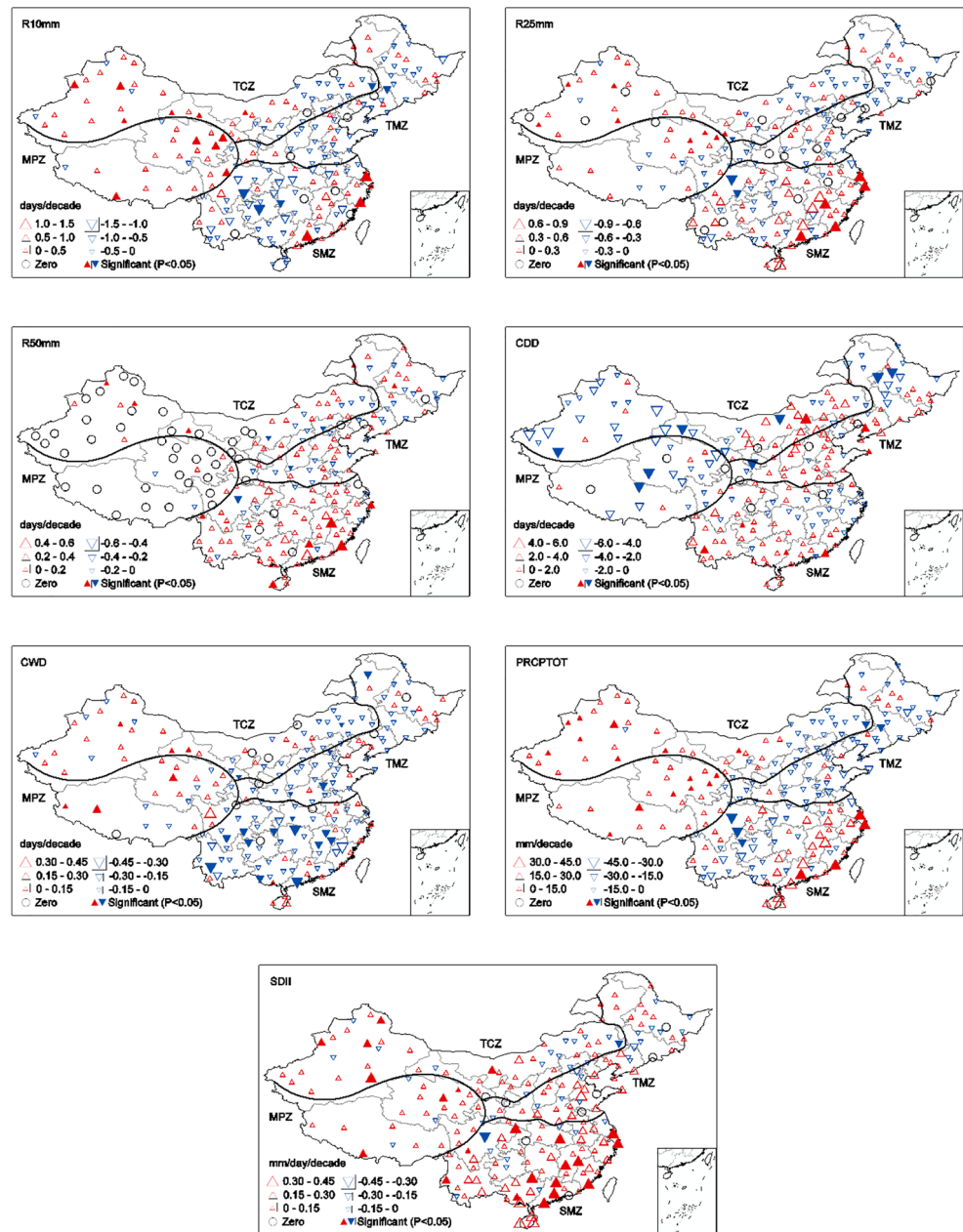
Fig. 8 Annual variations of spatially averaged values of threshold, duration, and other precipitation indexes during 1956–2015 across different climatic zones of China



frequency of precipitation extremes declined in southern, north-east, and northern China, while they increased in the western and southeastern coastal China (Zhai et al. 2005). Mei et al. (2018) have demonstrated that precipitation extremes decreased

in northern China during 1960–2013. This difference can be largely attributed to the fact that they did not consider the climatic change points, which further confirmed the importance of different time-series analyses of precipitation extremes.

Fig. 9 Spatial distributions of change trends (per decade) in threshold, duration, and other precipitation indexes in China during 1956–2015. Positive/negative trends are shown as up/down triangles, and the filled symbols represent statistically significant trends at the 0.05 level. The size of the triangles is proportional to the magnitude of the trends



4.2 Comparison of changes of temperature and precipitation extremes in contrasting climate zones of China

There were variations in the change magnitudes of extreme temperature and precipitation indexes across different regions of China. For most temperature extremes, stations in the mountain plateau zone (MPZ) tended to exhibit the largest trend magnitudes, and stations in the (sub) tropical monsoon zone (SMZ) had the smallest trend magnitudes. As for some warm extremes, TN90p, TX90p, SU25, TR20, and WSDI also increased profoundly in SMZ. The differences in the spatial pattern of extreme temperature indexes were also

found by previous researchers. Liu et al. (2004) analyzed daily temperature data in China from 1955 to 2000 and found that temperature extremes showed increasing trends and the increased temperatures were most remarkable in northwestern China and were the lowest in the southwest. Xu et al. (2011) concluded that obvious decreases of cool nights/days were observed in northern and northeastern China, whereas warm nights/days increased remarkably in southern, southwestern, and northwestern China. Compared with the studies of Wang et al. (2013a) and (2013b) on climatic extremes in northwestern China and over the western Tibetan Plateau, it was found that the trends of temperature extremes appeared to have greater increases in the Tibetan

Plateau of China. Also, the decrease of frequency in cold extremes and the increase of frequency in warm extremes in the Tibetan Plateau were greater than those in eastern China (Yin and Sun 2018). This uneven spatial distribution can be ascribed to the comprehensive influences of global warming, atmospheric circulation oscillations, urbanization, topography, and elevation (Liu et al. 2009). The greatest warming trend in MPZ was most likely caused by the high elevation (average 4236 m a.s.l.), which agreed with the findings of Guan et al. (2015), who discovered that the climate warming was more significant at sites with greater altitudes compared with those with smaller altitudes. The higher the elevation was, the more notable decreases in cold-related indexes occurred when the elevation was larger than 350 m. Besides, the cloud-radiation and snow-albedo feedbacks were also regarded as other influencing factors in the Tibetan Plateau (Liu et al. 2009), which is an important part of MPZ. As elevation increases, the decreasing trend of total cloud amount and annual mean snow depth and the increasing trend of surface-absorbed solar radiation become more prominent, providing an explanation for the greater warming trend in MPZ in the present study. However, in the study of You et al. (2008), elevation had no obvious effect on the change of temperature indexes apart from TX10p and TXn. Some studies have also found the relationships between warming amplitude and latitude around the world. IPCC (2007) pointed out that warming was more obvious at high latitudes in the northern hemisphere under global warming. Guan (2015) found that the warming rate decreased with the decrease in latitude, which may result in the smallest warming amplitude in SMZ due to much lower latitudes in our study. In addition, greater warming trend was found at stations located around the coastline of SMZ, such as Jiangsu, Zhejiang, and Fujian provinces, although they had lower elevation but the same latitude compared with some inland provinces such as Sichuan and Guizhou provinces. This may be related to the rapid urbanization occurred in southeastern China (Zhou et al. 2004). Atmospheric circulation oscillations, such as El Niño-Southern Oscillation (ENSO), Arctic oscillation (AO), and North Atlantic Oscillation (NAO), may exert an important influence on temperature extremes. Thompson and Wallace (2001) found that the continuous change of NAO towards a high index was an important reason for winter warming in the northern hemisphere continental regions in recent decades. Ju et al. (2004) considered that AO possibly caused the anomaly of atmospheric circulation and the temperature increasing in North of East Asia Winter. The detailed influences of those factors on global warming in various regions require further study in the future.

Similar to temperature extremes, the change magnitudes of extreme precipitation indexes in different regions of China also varied. Precipitation extremes in TCZ and TMZ showed negative trends during 1956–1985, coupled

with the rise of consecutive dry days (CDD). However, the two regions were dominated by increasing trends of precipitation totals after 1985, indicating drought-induced disasters could be reduced in these regions. Shi et al. (2007) revealed that the climate in northwestern China changed from dryer to wetter in 1987. Wang et al. (2013a) suggested that precipitation indexes mostly exhibited a positive trend in northwestern China after 1986, indicating that the arid region of China was becoming wetter although this change was insignificant. Also, there was a generally downward trend in TMZ for CDD, and an upward trend for consecutive wet days (CWD) was observed in this region after 1985 (Table 4), which further confirmed the easing of droughts in TMZ in recent 30 years. Negative trends in CDD and positive trends in CWD were the strongest in the western part of TCZ and MPZ (Fig. 9), which indicated that precipitation is expected to occur more frequently in these regions, although they are not becoming heavier. Fu et al. (2008) also showed that the number of light rain days in western China had been increasing from 1961 to 2005. In general, the change magnitudes of R95p, R99p, RX1day, RX5day, R25mm, and R50mm were largest in SMZ, and stations having significantly enhancing trend were largely distributed in the southeastern coastal area of SMZ, which was similar to the findings of Ma et al. (2015), who pointed out that the averaged precipitation amount and days were largest in southeastern China. Besides, CWD showed a significantly downward trend and accompanied by the increase of CDD in the region of SMZ, but daily rainfall intensity (SDII) showed a significantly upward trend. Gao et al. (2017) analyzed the spatiotemporal variation of precipitation extremes in the monsoon region of China and found that the increasing trend of PRCPTOT was dominantly spread in the central-eastern China and southeastern coastal regions. These regions were characterized by declining trends in CWD and upward trends in SDII. In the study of Song et al. (2011), the number of precipitation days with light rainfall clearly decreased, while the precipitation days with heavy rain, often inducing floods, increased. Recent projection studies have shown that more frequent and more intense precipitation extremes would occur in the middle and lower reaches of the Yangtze River and the southeastern region (Feng et al. 2011b; Jiang et al. 2012b; Guo et al. 2018) by the end of the twenty-first century. One implication of this change is that the risk for floods in southern China would increase. Previous studies showed that atmospheric circulations oscillations had substantial influences on the variability of precipitation over China in a warming climate. The relationship of El Niño-Southern Oscillation (ENSO) and extreme rainfall in China varied in different regions and on various time scales (Fu et al. 2013). Huang and Wu

(1989) found droughts may become more common in northern China, while floods would occur over the Yangtze and Huaihe River Basins at the developing stage of El Niño. The Pacific decadal oscillation (PDO) plays an important role in regulating ENSO events, which affects the atmospheric circulation anomalies in Asia (Zhu and Yang 2003). The positive phase of Atlantic multidecadal oscillation (AMO) is usually related to higher monsoon over the monsoon region in China, while the phase of AMO index is reversed to provide negative anomalies of summer rainfall (Gao et al. 2017). The ENSO and AMO have an important influence on the East Asian summer monsoon (EASM) (Feng et al. 2011a; Gao et al. 2017). The EASM caused decreasing rainfall occurrence in central and southern North China, but increasing frequent occurrences of precipitation extremes over the lower and middle of the Yangtze River (Ding et al. 2008). However, Shi et al. (2018) suggested that the variability of precipitation indices were not significantly related to the circulation patterns in the vast majority of China. Apart from circulation patterns, land use may also have an impact on changes in extreme daily precipitation (Bornstein and Lin 2000; Jiang and Liu 2007; Pei et al. 2018). However, the detailed physical mechanisms need further study.

4.3 Influences of temperature and precipitation extremes on future agricultural production

Climate plays a key role in the development of agriculture. Assessment of the spatiotemporal variation of temperature and precipitation extremes are beneficial to further understanding the effects of climatic extremes on future agricultural production across the whole China. Our results indicated that precipitation totals in TCZ and TMZ have decreased by -10.97 and -17.52 mm/decade during 1956–1985, respectively, which may aggravate the regional water scarcity and lead to severe adverse influences on food productivity, particularly in the dryland area of these two regions. Increasing trends of precipitation in TCZ and TMZ were found after 1985, which may alleviate the pressure of agricultural water use to some extent. In our study, a continuous warming tendency was found across all climatic zones of China over the past six decades, especially during the recent 30-year period. Increasing temperature and extreme heat may evaporate more soil water and inhibit crop growth. For instance, increasing temperature will alter the evapotranspiration in arid and semi-arid regions, which will further intensify the water scarcity in these areas (Fan et al. 2016). The warming climate may suppress the increase of crop yield in northern, northwestern, and southwestern China due to the aggravation of water shortage (Li et al. 2019). Farmers are suggested to choose crops with better resilience to drought in this situation. However, the warming trend in northeastern China is generally advantageous to agricultural production because of the shortened frost

days, extended summer days, and longer growing season length (Yu and Li 2015). It is thus recommended to replace the early–medium crop ripeness with the medium–late ripeness variety (Zhao 2010). In the areas with high risk of flood generation such as SMZ, it is necessary to adopt waterlogging-tolerant crop varieties to better meet the challenge of increasing total precipitation together with an increased frequency of heavy rainfall events in this region. The impact of climate change on agriculture production would be complex and ambiguous. Thus, further research is required to explore the detailed effects of temperature and precipitation extremes on crop growth and yield in the context of ongoing climate warming in contrasting climate zones of China.

5 Conclusions

Understanding the spatiotemporal trends of extreme temperature and precipitation events in the context of continued global warming is of significance for agricultural production and water resources management. Based on 200 representative weather stations in contrasting climate zones of China over the span of 1956–2015, spatiotemporal trends and rates of temperature and precipitation extremes were studied using the Mann–Kendall test, Sen's slope estimator, and the Pettitt test. The results showed that temperature extremes exhibited large correlations with annual mean air temperature and all extreme temperature indexes had consistently warming trends in the whole China. The most remarkable change of temperature extremes was detected in MPZ and the smallest change magnitude occurred in SMZ. Acceleration in warming was especially identified after 1985. Nationally, changes in precipitation extremes during 1956–2015 showed lower significance, and only the trend of SDII was significant. Apart from consecutive wet days (CWD), the other extreme precipitation indexes indicated a wetting trend. In general, precipitation totals increased in MPZ and the western part of TCZ, which may alleviate the pressure of water-shortage in these arid and semi-arid regions. Nevertheless, the upward trend in SMZ, especially in the southeastern coastal areas of China, may aggravate the risk of floods in these regions. Regionally averaged extreme precipitation indexes showed decreasing trends in TMZ during 1956–1985, but upward trends were found after 1985. The results can provide a guideline for food production and eco-environment management strategy across contrasting climate zones of China.

Acknowledgments The authors extend their gratitude to the National Meteorological Information Center of China Meteorological Administration for offering the meteorological data.

Funding information This study was jointly financially supported by the National Natural Science Foundation of China (No. 51879226) and the “111” Project (B12007).

References

- Alexander LV, Zhang XB, Peterson TC, Caesar J, Gleason B, Klein Tank A, Haylock M, Collins D, Trewin B, Rahimzadeh F (2006) Global observed changes in daily climate extremes of temperature and precipitation. *J Geophys Res Atmos* 111(D05109)
- Bornstein R, Lin QL (2000) Urban heat islands and summertime convective thunderstorms in Atlanta: three case studies. *Atmos Environ* 34(3):507–516
- Castex V, Beniston M, Calanca P, Fleury D, Moreau J (2018) Pest management under climate change: the importance of understanding tritrophic relations. *Sci Total Environ* 616–617:397–407
- Cheong WK, Timbal B, Golding N, Sirabaha S, Kwan KF, Cinco TA, Han S (2018) Observed and modelled temperature and precipitation extremes over Southeast Asia from 1972 to 2010. *Int J Climatol* 38(7):3013–3027
- Choi G, Collins D, Ren GY, Trewin B, Baldi M, Fukuda K, Afzaal M, Pianmana T, Gomboluudev P, Huong PTT, Lias N, Kwon WT, Boo KO, Cha YM, Zhou YQ (2009) Changes in means and extreme events of temperature and precipitation in the Asia-Pacific Network region, 1955–2007. *Int J Climatol* 29:1906–1925
- Ding YH, Wang ZY, Sun Y (2008) Inter-decadal variation of the summer precipitation in East China and its association with decreasing Asian summer monsoon. Part I: observed evidences. *Int J Climatol* 28:1139–1161
- Ding T, Gao H, Li WJ (2018) Extreme high-temperature event in southern China in 2016 and the possible role of cross-equatorial flows. *Int J Climatol* 38(9):3579–3594
- Dookie N, Xsitaaz TC, Ricardo MC (2019) Trends in extreme temperature and precipitation indices for the Caribbean small islands: Trinidad and Tobago. *Theor Appl Climatol* 136(1–2):31–44
- Fan JL, Wu LF, Zhang FC, Xiang YZ, Zheng J (2016) Climate change effects on reference crop evapotranspiration across different climatic zones of China during 1956–2015. *J Hydrol* 542:923–937
- Fan JL, Yue WJ, Wu LF, Zhang FC, Cai HJ, Wang XK, Lu XH, Xiang YZ (2018) Evaluation of SVM, ELM and four tree-based ensemble models for predicting daily reference evapotranspiration using limited meteorological data in different climates of China. *Agric For Meteorol* 263:225–241
- Fan JL, Wu LF, Zhang FC, Cai HJ, Ma X, Bai H (2019) Evaluation and development of empirical models for estimating daily and monthly mean daily diffuse horizontal solar radiation for different climatic regions of China. *Renew Sust Energ Rev* 105:168–186
- Feng J, Chen W, Tam CY, Zhou W (2011a) Different impacts of El Niño and El Niño Modoki on China rainfall in the decaying phases. *Int J Climatol* 31:2091–2101
- Feng L, Zhou TJ, Wu B, Li T, Luo JJ (2011b) Projection of Future Precipitation Change over China with a High-Resolution Global Atmospheric Model. *Adv Atmos Sci* 28(2):464–476
- Fu QL, Lin X, Qian WH (2008) The temporal and spatial characteristics of graded summer rain days over China. *J Trop Meteorol* 24:367–373
- Fu GB, Yu JJ, Yu XB, Ouyang RL, Zhang YC, Wang P, Liu WB, Min LL (2013) Temporal variation of extreme rainfall events in China, 1961–2009. *J Hydrol* 487:48–59
- Gao T, Judy Wang HX, Zhou TJ (2017) Changes of extreme precipitation and nonlinear influence of climate variables over monsoon region in China. *Atmos Res* 197:379–389
- Gocic M, Trajkovic S (2013) Analysis of changes in meteorological variables using Mann-Kendall and Sen's slope estimator statistical tests in Serbia. *Glob Planet Chang* 100:172–182
- Guan YH (2015) Extreme climate change and its trend prediction in the Yangtze River Basin (Ph.D). Northwest A&F University, Yangling
- Guan YH, Zhang XC, Zheng FL, Wang B (2015) Trends and variability of daily temperature extremes during 1960–2012 in the Yangtze River Basin, China. *Glob Planet Chang* 124:79–94
- Guo ZF, Liu JQ (2002) Research advance in effect of volcanism on climate changes. *Adv Earth Science* 17:595–604 (in Chinese)
- Guo JH, Huang GH, Wang XQ, Li YP, Yang L (2018) Future changes in precipitation extremes over China projected by a regional climate model ensemble. *Atmos Environ* 188:142–156
- Harrison L, Michaelsen J, Funk C, Husak G (2011) Effects of temperature changes on maize production in Mozambique. *Clim Res* 46:211–222
- Huang RH, Wu YF (1989) The influence of ENSO on the summer climate change in China and its mechanism. *Adv Atmos Sci* 6:21–32
- IPCC (2007) Summary for Policymakers of Climate Change, 2007: The physical science basis. In: Contribution of working group I to the fourth assessment report of the intergovernmental panel on climate change. Cambridge University Press, Cambridge
- IPCC (2013) Climate change, 2013: the physical science basis. In: Contribution of working group I to the fifth assessment report of the intergovernmental panel on climate change. Cambridge University Press, Cambridge, p 1535
- Jiang X, Liu WD (2007) Numerical simulations of impacts of urbanization on heavy rainfall in Beijing using different land-use data. *J Met Res* 21(2):245–255
- Jiang FQ, Hu RJ, Wang SP, Zhang YW, Tong L (2012a) Trends of precipitation extremes during 1960–2008 in Xinjiang, the Northwest China. *Theor Appl Climatol* 111:133–148
- Jiang ZH, Song J, Li L, Chen WL, Wang ZF, Wang J (2012b) Extreme climate events in China: IPCC-AR4 model evaluation and projection. *Clim Chang* 110:385–401
- Ju JH, Ren JZ, Lv JM (2004) Effect of interdecadal variation of Arctic oscillation on temperature increasing in north of East Asian winter. *Plateau Meteorol* 23(4):429–434 (in Chinese)
- Kendall MG (1975) Rank correlation methods. Griffin, London
- Li HX, Chen HP, Wang HJ (2017) Effects of anthropogenic activity emerging as intensified extreme precipitation over China. *J Geophys Res Atmos* 122(13):6899–6914
- Li LC, Yao N, Li Y, Liu DL, Wang B, Ayantobo OO (2019) Future projections of extreme temperature events in different sub-regions of China. *Atmos Res* 217:150–164
- Liu BH, Xu M, Henderson M, Qi Y (2004) Taking China's temperature: daily range, warming trends, and regional variations. *J Clim* 17(22):4453–4462
- Liu XD, Cheng ZG, Yan LB, Yin ZY (2009) Elevation dependency of recent and future minimum surface air temperature trends in the Tibetan Plateau and its surroundings. *Glob Planet Chang* 68:164–174
- Liu SY, Huang SZ, Xie YY, Huang Q, Leng GY, Hou BB, Zhang Y, Wei X (2018) Spatial-temporal changes of maximum and minimum temperatures in the Wei River Basin, China: changing patterns, causes and implications. *Atmos Res* 204:1–11
- Liu XW, Xu ZX, Peng DZ, Wu GC (2019) Influences of the North Atlantic Oscillation on extreme temperature during the cold period in China. *Int J Climatol* 39(1):43–49
- Lu CH, Sun Y, Wan H, Zhang XB, Yin H (2016) Anthropogenic influence on the frequency of extreme temperatures in China. *Geophys Res Lett* 43(12):6511–6518
- Ma SM, Zhou TJ, Dai AG, Han ZY (2015) Observed Changes in the distributions of daily precipitation frequency and amount over China from 1960 to 2013. *J Clim* 28:6960–6978
- Mann HB (1945) Nonparametric tests against trend. *Econometrica* 13:245–259
- Mei C, Liu JH, Chen MT, Wang H, Li M, Yu YD (2018) Multi-decadal spatial and temporal changes of extreme precipitation patterns in northern China (Jing-Jin-Ji district, 1960–2013). *Quat Int* 476:1–13

- Pachauri RK, Allen MR, Barros VR, Broome J, Cramer W, Christ R, Church JA, Clarke L, Dahe Q, Dasgupta P, Dubash NK, Edenhofer O, Elgizouli I, Field CB, Forster P, Friedlingstein P, Fuglestedt J, Gomez-Echeverri L, Hallegatte S, Hegerl G, Howden M, Jiang K, Jimenez Cisneros B, Kattsov V, Lee H, Mach KJ, Marotzke J, Mastrandrea MD, Meyer L, Minx J, Mulugetta Y, O'Brien K, Oppenheimer M, Pereira JJ, Pichs-Madruga R, Plattner GK, Pörtner HO, Power SB, Preston B, Ravindranath NH, Reisinger A, Riahi K, Rusticucci M, Scholes R, Seyboth K, Sokona Y, Stavins R, Stocker T F, Tschakert P, van Vuuren D, van Ypersele JP (2014) Climate change 2014: synthesis report. Contribution of working groups I, II and III to the fifth assessment report of the intergovernmental panel on climate change. IPCC, Geneva, p 151
- Pei FS, Wu CJ, Liu XP, Hu ZL, Xia Y, Liu LA, Wang K, Zhou Y, Xu L (2018) Detection and attribution of extreme precipitation changes from 1961 to 2012 in the Yangtze River Delta in China. *Catena* 169: 183–194
- Pettitt AN (1979) A non-parametric approach to the change-point problem. *J R Stat Soc* 28(2):126–135
- Rodgers LJ, Nicewander WA (1988) Thirteen ways to look at the correlation coefficient. *Am Stat* 42(1):59–66
- Ruml M, Gregorić E, Vujadinović M, Radovanović S, Matović G, Vuković A, Počuča V, Stojičić D (2017) Observed changes of temperature extremes in Serbia over the period 1961–2010. *Atmos Res* 183:26–41
- Sen PK (1968) Estimates of the regression coefficient based on Kendall's tau. *J Am Stat Assoc* 63:1379–1389
- Shi YF, Shen YP, Kang E, Li DL, Ding YJ, Zhang GW, Hu RJ (2007) Recent and future climate change in northwest China. *Clim Chang* 80(3–4):379–393
- Shi J, Cui LL, Wang JB, Du HQ, Wen KM (2018) Changes in the temperature and precipitation extremes in China during 1961–2015. *Quat Int*. <https://doi.org/10.1016/j.quaint.2018.08.008>
- Song YL, Achberger C, Linderholm HW (2011) Rain-season trends in precipitation and their effect in different climate regions of China during 1961–2008. *Environ Res Lett* 6:34025
- Sun WY, Mu XM, Song XY, Wu D, Cheng AF, Qiu B (2016) Changes in extreme temperature and precipitation events in the Loess Plateau (China) during 1960–2013 under global warming. *Atmos Res* 168: 33–48
- Thompson DWJ, Wallace JM (2001) Regional climate impacts of the Northern Hemisphere annular mode. *Science* 293:85–89
- Voitikhovich OV, Kanivets V, Onishi Y (2007) The Chernobyl accident and its aquatic impacts on the surrounding area. In: Onishi Y, Voitikhovich OV, Zheleznyak MJ (eds) Chernobyl-what have we learned? Environmental Pollution, vol 12. Springer, Dordrecht
- Wang HJ, Chen YN, Xun S, Lai DM, Fan YT, Li Z (2013a) Changes in daily climate extremes in the arid area of northwestern China. *Theor Appl Climatol* 112:15–28
- Wang SJ, Zhang MJ, Wang BL, Sun MP, Li XF (2013b) Recent changes in daily extremes of temperature and precipitation over the western Tibetan Plateau, 1973–2011. *Quat Int* 313–314:110–117
- Wang XL, Hou XY, Wang YD (2017) Spatiotemporal variations and regional differences of extreme precipitation events in the Coastal area of China from 1961 to 2014. *Atmos Res* 197:94–104
- Wang G, Yan DH, He XY, Liu SH, Zhang C, Xing ZQ, Kan GY, Qin TL, Ren ML, Li H (2018) Trends in extreme temperature indices in Huang-Huai-Hai River basin of China during 1961–2014. *Theor Appl Climatol* 134(1–2):51–65
- Xu X, Du YG, Tang JP, Wang Y (2011) Variations of temperature and precipitation extremes in recent two decades over China. *Atmos Res* 101:143–154
- Xu M, Kang SC, Wu H, Yuan X (2018) Detection of spatio-temporal variability of air temperature and precipitation based on long-term meteorological station observations over Tianshan Mountains, Central Asia. *Atmos Res* 203:141–163
- Yin H, Sun Y (2018) Characteristics of extreme temperature and precipitation in China in 2017 based on ETCCDI indices. *Adv Clim Chang Res* 9(4):218–226
- You QL, Kang SC, Aguilar E, Yan Y (2008) Changes in daily climate extremes in the eastern and central Tibetan Plateau during 1961–2005. *J Geophys Res* 113(D07101)
- Yu Z, Li XL (2015) Recent trends in daily temperature extremes over northeastern China (1960–2011). *Quat Int* 380–381:35–48
- Zhai PM, Zhang XB, Wan H, Pan XH (2005) Trends in total precipitation and frequency of daily precipitation extremes over China. *J Clim* 18(7):1096–1108
- Zhang XB, Yang F (2004) RCLimDex (1.0) User Manual. Climate Research Branch, Environment Canada, Ontario
- Zhao XL (2010) Influence of climate change on agriculture in Northeast China in recent 50 years. *J Northeast Agric Univ* 41(9):144–149 (in Chinese)
- Zhou LM, Dickinson RE, Tian YH, Fang JY, Li QX, Kaufmann RK, Tucker CJ, Myneni RB (2004) Evidence for a significant urbanization effect on climate in China. *PNAS* 101:9540–9544
- Zhou BT, Xu Y, Wu J, Dong SY, Shi Y (2016) Changes in temperature and precipitation extreme indices over China: analysis of a high-resolution grid dataset. *Int J Climatol* 36:1051–1066
- Zhu YM, Yang XQ (2003) Relationships between Pacific decadal oscillation (PDO) and climate variability in China. *J Meteorol Res-Prc* 61(6):641–654

Publisher's note Springer Nature remains neutral with regard to jurisdictional claims in published maps and institutional affiliations.